Studies of Heisenberg Spin Exchange in ESR Spectra. I. Linewidth and Saturation Effects*

M. P. EASTMAN,† R. G. KOOSER,‡ M. R. DAS, AND J. H. FREED§
Department of Chemistry, Cornell University, Ithaca, New York 14850

(Received 24 March 1969)

A compact general theory for the effect of Heisenberg spin exchange on ESR linewidths and saturation parameters is detailed. The effects of Heisenberg exchange on the linewidths of the tetracyanoethylene anion ($TCNE^-$) radical and the di-*tert*-butyl nitroxide (DTBN) radical in both dimethoxyethane (DME) and tetrahydrofuran (THF) are investigated. From comparative studies of linewidth as a function of temperature and of radical concentration, $TCNE^-$ in DME is shown to undergo strong exchange with a second-order rate constant of $4.1\pm0.6\times10^9 M^{-1}\cdot\sec^{-1}$ at 15°C. The $TCNE^-$ radical in THF exhibits an anomalous concentration-dependent linewidth effect when compared to the theory and to the experiments employing DME as the solvent. The uncharged DTBN radical shows similar spin-exchange properties in both solvents. Possible mechanisms for the anomalous linewidth effect are discussed. The effect of spin exchange on the saturation parameters of the $TCNE^-$ radical in DME is investigated in detail, and the experimental results are shown to agree, within experimental error, with the theory developed. Electron–nuclear dipolar and electron–electron dipolar relaxation effects are discussed in terms of their (small) contributions to the experimentally determined relaxation times.

I. INTRODUCTION

Heisenberg spin exchange, in which two free radicals exchange their spins during an encounter, may in a large sense be regarded as a very simple chemical reaction requiring no rearrangement or transfer of masses. From that point of view, it is a phenomenon worthy of study for purposes of comparison with more conventional and more complex types of chemical reactions.

There have already been several experimental ESR studies of spin exchange in liquids,[1–7] which have, for the most part, assumed that the effects of spin exchange on ESR linewidths are essentially those of a largely diffusion-controlled chemical exchange process. A more careful theoretical analysis of the phenomenon has been developed by several authors[8–11] since the initial discussion given by Pake and Tuttle.[12] In a preliminary report,[10] one of us has shown that under a variety of conditions the effects of Heisenberg spin exchange on ESR spectra will be identical to those of chemical exchange (and not necessarily diffusion controlled), and on this basis a detailed theoretical analysis was developed for a variety of linewidth and saturation effects of exchange.[13] A more detailed account of the theoretical aspects relating to linewidths but not saturation phenomena and yielding results very similar to those reported in Ref. 10, has been given independently by Johnson,[11] and conforms to the earlier theory of Currin.[9]

One major objective of the present work was to compare the linewidth and saturation effects of spin exchange in order to confirm the theoretical predictions of Ref. 13, based on the nonsecular type of behavior of the process as noted in Ref. 10. There does not appear to have been any previous saturation study of spin exchange in liquids. Such a study also allows an unequivocal demonstration of effects of coupled relaxation of hyperfine lines upon saturation behavior. It was also deemed important to carefully confirm other characteristics of spin-exchange effects as predicted by the theory to serve as a basis for further explorations on this phenomenon.

The radical potassium tetracyanoethylene (K^+ $TCNE^-$) was chosen for these studies for several reasons. It can be isolated as a stable pure salt (92%–100% pure in these studies), and in many solutions it remains stable for long periods of time. In the absence of exchange, it gives a simple well-resolved spectrum of Lorentzian lines from the four equivalent ^{14}N nuclei, and in solvents of low viscosity yields intensity ratios very close to the theoretically expected 1:4:10:16:19:16:10:4:1.[14] This latter condition is important, because it implies that intramolecular electron–nuclear dipolar

* Supported in part by Public Health Service Research Grant No. GM 14123 from the National Institutes of Health and by the Advanced Research Projects Agency.

† NIH Predoctoral Fellow, 1967–1968. Gulf Oil Fellow, 1966–1967. Present address: University of California, Los Alamos Scientific Laboratory, Los Alamos, N.M. 87544.

‡ NIH Predoctoral Fellow 1967–1968. Present address: Department of Chemistry, Knox College, Galesburg, Ill.

§ Alfred P. Sloan Foundation Fellow, 1966–1968.

[1] M. T. Jones, J. Chem. Phys. **38,** 2892 (1963).

[2] T. A. Miller, R. N. Adams, and P. M. Richards, J. Chem. Phys. **44,** 4022 (1966).

[3] T. A. Miller and R. N. Adams, J. Am. Chem. Soc. **88,** 5713 (1966).

[4] J. G. Powles and M. H. Mosley, Proc. Phys. Soc. (London) **78,** 370 (1961).

[5] J. C. Danner and T. R. Tuttle, Jr., J. Am. Chem. Soc. **85,** 4052 (1963).

[6] W. Plachy and D. Kivelson, J. Chem. Phys. **47,** 3312 (1967).

[7] N. Edelstein, A. Kwok, and A. H. Maki, J. Chem. Phys. **41,** 3473 (1964).

[8] D. Kivelson, J. Chem. Phys. **33,** 1094 (1960).

[9] J. D. Currin, Phys. Rev. **126,** 1995 (1962).

[10] J. H. Freed, J. Chem. Phys. **45,** 3452 (1966).

[11] C. S. Johnson, Mol. Phys. **12,** 25 (1967).

[12] G. E. Pake and T. R. Tuttle, Jr., Phys. Rev. Letters **3,** 423 (1959).

[13] J. H. Freed, J. Phys. Chem. **71,** 38 (1967).

[14] J. Gendell, J. H. Freed, and G. K. Fraenkel, J. Chem. Phys. **41,** 949 (1964). We have replaced the symbol $\tilde{M}$, as used by these authors, by M for convenience.

(END) relaxation should not be very significant in affecting the exchange studies, particularly the saturation work. Finally, it was found that $TCNE^-$ undergoes simple and strong exchange which is easily characterized by its T/η (temperature/viscosity) dependence. This was expected, because in the solid K^+TCNE^- is a ground-state singlet with the associated excited triplet state separated by the substantial exchange interaction $J=0.26$ eV.[15] The $TCNE^-$ radical was deemed a more satisfactory choice than any of the radicals previously studied because none of the latter offered all these desirable characteristics.

Since only a partial description of the relevant relaxation theory has been presented,[10,13] an account utilizing a compact operator approach is given here which emphasizes the fact that Heisenberg spin exchange is a chemical-exchange-type process from the point of view of ESR observables. It was also necessary to find a general expression of exchange effects on saturation parameters for many-line spectra, as the few simple cases considered earlier[13] are inadequate for the $TCNE^-$ work.

Besides these objectives, it was felt that there would be a number of interesting features of the K^+TCNE^- system in particular. Unlike the di-*tert*-butyl nitroxide (DTBN) radical for which systematic studies of the effects of solvent and T/η have been made,[6,7] $TCNE^-$ is a charged radical and this could influence the exchange behavior as evidenced in solvent- and T/η dependent studies. Also, it is a prototype for a strong exchange interaction as opposed to the interesting not-so-strong exchange interaction exhibited by DTBN in some solvents as analyzed by Plachy and Kivelson.[6] Thus linewidth studies both of $TCNE^-$ and of DTBN (for comparison) were made in dimethoxyethane (DME) and tetrahydrofuran (THF) solvents. The comparison yielded an anomalous linewidth observation for the $TCNE^-$:THF system.

A review of the theory including our new and more detailed results appears in Sec. II. The experimental methods are described in Sec. III. The linewidth and saturation results are given in Secs. IV and V, respectively, and are discussed in Sec. VI. The possibly complicating effects of intermolecular electron–electron dipolar and END interactions are analyzed in Appendices C and D, respectively.

II. THEORETICAL ANALYSIS

A. Density-Matrix Treatment

We start by utilizing Lynden-Bell's approach.[10,16] The density matrix equation for the radical monomers is

$$i\dot{\rho}=[H_T^{(1)},\rho]+i(2/\tau_2)\ \mathrm{Tr}\,\sigma-i(2/\tau_2)\rho, \qquad (2.1)$$

where τ_2 is the mean time between successive new bimolecular encounters of radicals, $H_T^{(1)}$ is the spin Hamiltonian, and

$$\mathrm{Tr}_s\sigma=\tfrac{1}{2}(\mathrm{Tr}_1\sigma+\mathrm{Tr}_2\sigma) \qquad (2.2)$$

is a symmetrized trace over each of the two components of the interacting dimer, which is characterized by spin-density matrix σ. It obeys the equation of motion,

$$i\dot{\sigma}=[H_T^{(1)}+H_T^{(2)}+H_J,\sigma]-i\tau_1^{-1}\sigma+i\tau_1^{-1}\rho\times\rho, \qquad (2.3)$$

where H_J is the exchange interaction and τ_1 is the mean lifetime of the collision pair. The appropriate spin Hamiltonians, in the frame rotating with the microwave field of frequency ω, are

$$H_T^{(1)}=(\omega_0-\omega)S_z^{(1)}+\sum_i a_i\mathbf{I}_i^{(1)}\mathbf{S}_i^{(1)}+\omega_{1s}S_x^{(1)}, \qquad (2.4a)$$

$$H_J=J\mathbf{S}^{(1)}\cdot\mathbf{S}^{(2)}. \qquad (2.4b)$$

Here J is twice the exchange integral, ω_0 the Larmour frequency of the electron spins, a_i the hyperfine interaction of the ith magnetic nucleus, and ω_{1s} the interaction of microwave field with the electron spin. In the rotating frame σ takes on the steady-state, time-independent value ($\dot{\sigma}=0$),

$$\begin{aligned}\sigma&=(H_T^{(1)x}+H_T^{(2)x}+H_J{}^x-i/\tau_1)^{-1}(i/\tau_1)\rho\times\rho\\&=(\tilde{H}^x-i/\tau_1)^{-1}(i/\tau_1)\rho\times\rho,\end{aligned} \qquad (2.5)$$

where we have introduced the notation that for any two operators A and B, $A^xB\equiv[A,B]$. A substitution of Eq. (2.5) into Eq. (2.1) followed by a simple rearrangement then leads to

$$i\dot{\rho}=H_T^{(1)x}\rho+(2i/\tau_2)\ \mathrm{Tr}\,[(\tilde{H}^x-i/\tau_1)^{-1}\tilde{H}^x(\rho\times\rho)]. \qquad (2.6)$$

Equation (2.6) represents the formal operator solution for ρ, and when $\tau_2/\tau_1\gg1$ (i.e., very low concentration of dimers) spectral observables are well approximated by just considering the contribution from ρ. One may now take matrix elements of Eq. (2.6) and solve the coupled algebraic equations which ensue. However, it is possible to take advantage of the general properties of H_J to proceed further with the operator solution provided certain conditions, fulfilled in the work discussed here, are assumed. That is, we assume ω is near the resonance frequencies in the absence of exchange and[17]

$$|J|,\tau_1^{-1}\gg|a_i|;\omega_1, \qquad (2.7)$$

[15] D. B. Chestnut and W. D. Phillips, J. Chem. Phys. **35**, 1002 (1961).

[16] R. M. Lynden-Bell, Mol. Phys. **8**, 71 (1964).

[17] These conditions are actually somewhat more restrictive than necessary.[10] One finds from a careful analysis of the matrix elements of ρ [from Eq. (2.6)], which are important in ESR line broadening, that the result, Eq. (2.14), is also appropriate if just $\tau_1^{-1}\gg|a_s|,\omega_{1s}$, provided only that the slow-exchange condition $\omega_{HE}\ll|a_s|$ is fulfilled. This also follows from Johnson's treatment[11] when one combines his results for the two special cases for slow exchange: (1) $|a_s|,\ll|J|,\tau_1^{-1}$ and (2) $|a_sJ|\ll\tau_1^{-2}$ by recognizing that (2) is consistent with $|J|\lesssim|a_s|\ll\tau_1^{-1}$.

so that Eq. (2.6) is approximated by

$$i\dot{\rho}\cong H_T^{(1)x}\rho+(2i/\tau_2)\ \mathrm{Tr}_s[(H_J^x-i/\tau_1)^{-1}H_J^x(\rho\times\rho)]. \tag{2.8}$$

Now, since a constant matrix: $c\mathbf{1}$ commutes with any other matrix we may replace H_J^x in Eq. (2.8) by the commutator form of the operator,

$$(\tfrac{1}{2}J)P\equiv\tfrac{1}{2}J(\tfrac{1}{2}\mathbf{1}+2\mathbf{S}_1\cdot\mathbf{S}_2)=(\tfrac{1}{4}J)\mathbf{1}+H_J. \tag{2.9}$$

This operator P is a permutation operator which has the simple effect of exchanging spins between the interacting pair of electrons spins.[18] The coefficient $\frac{1}{2}J$ gives its magnitude relative to the other operators. Thus we have

$$P^2=1.^{19a} \tag{2.10}$$

Equation (2.10) leads to the relations

$$(P^x)^{2n}A=2^{(2n-1)}(A-PAP), \qquad n=1,2,3,\cdots, \tag{2.11}$$

$$(P^x)^{2n+1}A=2^{2n}p^xA, \qquad n=0,1,2,3,\cdots. \tag{2.12}$$

Now it is possible to expand the inverse operator $i\tau_1(1-\epsilon P^x)^{-1}$, where $\epsilon=-\frac{1}{2}iJ\tau_1$,

$$\begin{aligned}(1-\epsilon P^x)^{-1}A&=\frac{1+\epsilon P^x}{1-\epsilon^2(P^x)^2}A=A+\tfrac{1}{2}\sum_{n=1}^{\infty}(2\epsilon)^{2n}\\&\quad\times(A-PAP)+\tfrac{1}{2}\sum_{n=0}^{\infty}(2\epsilon)^{2n+1}(P^xA)\\&=\left[1+\frac{1}{4}\frac{(2\epsilon)^2}{1-(2\epsilon)^2}(P^x)^2\right.\\&\quad\left.+\frac{1}{2}\frac{2\epsilon}{1-(2\epsilon)^2}P^x\right]A, \quad \text{for} \quad |2\epsilon|<1.\end{aligned} \tag{2.13}$$

Thus, the series expansions are summable.[20] Now when Eq. (2.13) is utilized for Eq. (2.8) and Eqs. (2.11) and (2.12) are again employed, we obtain

$$\begin{aligned}i\dot{\rho}=H_T^{(1)x}\rho+i\omega_{\mathrm{HE}}[\mathrm{Tr}_s(P\rho\times\rho P)-\rho]\\+(J\tau_1)^{-1}\omega_{\mathrm{HE}}\ \mathrm{Tr}_s[P^x(\rho\times\rho)],\end{aligned} \tag{2.14}$$

where

$$\omega_{\mathrm{HE}}=(\tau_2)^{-1}[J^2\tau_1^2/(1+J^2\tau_1^2)]. \tag{2.15}$$

Now Eq. (2.14) is little more than the spin-density matrix equation of motion given by Kaplan[18] and Alexander[19b] for a simple chemical-exchange process involving molecules of a single species and with exchange frequency ω_{HE}. (In this case, the molecules are merely exchanging their electron spins.) The only difference is the added third term on the right, which corresponds to a frequency shift. It is possible to show that this last term is zero in the high-temperature approximation, i.e., when $N\rho\cong\mathbf{1}+\rho'$, where N is the number of spin eigenstates and ρ' is a small correction to the unit matrix.[20] This is outlined in Appendix A.

Now Eq. (2.14) was derived for $J<\tau_1^{-1}$, because this condition allowed us to obtain convergent expansions. However, since it is possible to sum the series, and obtain the result Eq. (2.14) which is analytic for all values of $J\tau_1$, one expects that by analytic continuation[21] the solution should be valid for all values of $J\tau_1$.[22] We thus conclude that in the high-temperature approximation, and given Eq. (2.7), Heisenberg exchange appears as a simple exchange process requiring only a single spin-density matrix ρ to which the methods of Alexander[19b] apply. This justifies the treatment of HE effects discussed in Ref. 13.

In the case of simple Brownian diffusion of the radicals in solution we can write[23–27]

$$\tau_2^{-1}=4\pi dDf\mathfrak{N} \tag{2.16a}$$

and

$$\tau_1^{-1}=(6D/d^2)fe^u, \tag{2.16b}$$

---

[18] J. I. Kaplan, J. Chem. Phys. **29,** 462 (1958).

[19] (a) S. Alexander, J. Chem. Phys. **37,** 966 (1962); (b) **37,** 974 (1962).

[20] One can show that the inverse of P^x cannot be a well-defined operator. This prevents utilizing any expansions in ϵ^{-1} for $|\epsilon|>1$.

[21] E. T. Whitaker and G. N. Watson [A Course of Modern Analysis (Cambridge University Press, New York, 1927), 4th ed., p. 96] discuss analytic continuation for ordinary functions.

[22] That this statement is true for the operator equations is most directly verified by solving Eq. (2.8) for specific matrix elements of ρ, which yields results such as those reported in Ref. 10. Actually, one can perform the derivation in a way that is valid for all $|J\tau_1|<\infty$ by a slightly more complicated procedure than that given above. We note Eq. (2.5), the steady-state limit of Eq. (2.3), could also have been obtained by first integrating Eq. (2.3) with respect to time t, and then letting $t\to\infty$. That is

$$\begin{aligned}\sigma(t\to\infty)=\{\exp[(-i\bar{H}^x-\tau_1^{-1})t\}\sigma(0)\\+\lim_{t\to\infty}\int_0^t\{\exp[(-i\bar{H}^x-\tau_1^{-1})(t-t')]\}\rho\times\rho dt',\end{aligned}$$

where $\sigma(0)$ is some initial value of $\sigma(t)$. The first term vanishes for $t/\tau\ll1$, while the second term yields Eq. (2.5). If, however, we first let $\bar{H}^x-i\tau_1^{-1}\cong\bar{H}_J^x-i\tau_1^{-1}$; then we expand $\exp[-i\bar{H}_J^x(t-t')]$ in a series making use of Eqs. (2.9)–(2.12), it is possible to resume the series in a manner analogous to Eqs. (2.13) but yielding a cosine and a sine function and valid for all values of $|J(t-t')|$. Then the integration and limit may be taken. A substitution of this result for $\sigma(t\to\infty)$ into Eq. (2.1), followed by a simple rearrangement yields Eq. (2.14). The second and third terms in Eq. (2.14) arise, respectively, from the cosine and sine terms.

[23] I. Amdur and G. G. Hammes, *Chemical Kinetics* (McGraw-Hill Book Co., New York, 1966), Chap. 2.

[24] P. Debye, Trans. Electrochem. Soc. **82,** 265 (1942).

[25] S. Chandrasekhar, Rev. Mod. Phys. **15,** 1 (1943).

[26] M. Eigen, Z. Physik. Chem. N.F. **1,** 176 (1954).

[27] This expression, unlike that given by J. S. Hyde, J. C. W. Chien, and J. H. Freed [J. Chem. Phys. **48,** 4211 (1968)], includes a factor of $\frac{1}{2}$ to avoid counting each collision twice, see S. W. Benson, *The Foundations of Chemical Kinetics* (McGraw-Hill Book Co., New York, 1960), pp. 154, 498.

where $\mathfrak{N}$ is the density of radicals, and the diffusion coefficient D in a Stokes–Einstein model is

$$D=kT/6\pi a\eta, \tag{2.17}$$

with η the solvent viscosity, a the molecular radius, and d is the "interaction distance" for exchange. $U(r)$ is the intermolecular potential energy of interaction, which for simple like charges in a medium of dielectric constant ϵ is $U(r)=Z^2e^2/\epsilon r$; then $f=u/(e^u-1)$ where $u=U(d)/kT$. The effect of $U\neq 0$ for like charges is to reduce τ_2^{-1} but to increase τ_1^{-1} for a given value of d. If the medium has a finite ionic strength, the expression for f is altered.[23,24] Steric factors can also reduce τ_2^{-1}.

For the radical solutions considered in this work $\eta\sim 0.5$ cP, $T\sim 273$°K, concentrations of $\sim 1\times 10^{-3}$ M, and typical values for d should be of the order of a molecular diameter (~ 6 Å). Therefore typical values of τ_1 and τ_2 (for concentrations of $\sim 10^{-3}$ M) are about 10^{-10} sec and 10^{-6}–10^{-7} sec, respectively, for neutral radicals, while for charged radicals the value of τ_2/τ_1 can be even greater.

B. Linewidths and Saturation Parameters

It has been shown that for steady-state ESR experiments, the spectra in the presence of saturation may be described in matrix notation by[13,28]

$$\mathbf{Z}''=\mathbf{M}^{-1}(-\mathbf{R}^{-1})\mathbf{Q}, \tag{2.18}$$

$$\mathbf{Z}'=(-\mathbf{R}^{-1})\mathbf{K}\mathbf{Z}'', \tag{2.19}$$

with

$$\mathbf{M}=\mathbf{1}+(\mathbf{R}^{-1}\mathbf{K})^2+(-\mathbf{R}^{-1})\mathbf{S}. \tag{2.20}$$

Here $\mathbf{Z}$ is a column vector with real and imaginary parts;

$$\mathbf{Z}=\mathbf{Z}'+i\mathbf{Z}''. \tag{2.21}$$

Each component of $\mathbf{Z}''$ and $\mathbf{Z}'$ corresponds, respectively, to an absorption and a dispersion mode of a particular spin transition which is excited as a result of the applied rf fields. In a typical ESR experiment with multiple hyperfine lines, one can speak of "degenerate transitions" which are excited. It was shown in Ref. 13 that when the strongest nuclear spin-dependent relaxation processes are due to exchange, it is permissible to simplify the solution by summing over these degenerate transitions as well as over degenerate states. Thus we have

$$\bar{Z}_\lambda=\sum_j Z_{\lambda j}, \tag{2.22a}$$

$$\bar{\chi}_{\lambda\pm}=\sum_j \chi_{\lambda j}\pm, \tag{2.22b}$$

which are, respectively, sums over (2.22a) the Z components for the λth degenerate transition, and (2.22b) the diagonal density-matrix elements (actually their deviations from thermal equilibrium value) for the states between which these transitions occur. Then with the assumption of slow exchange

$$\omega_{\rm HE}\ll|\,a_i\,|, \tag{2.23}$$

the linewidth matrix $\mathbf{R}$ becomes diagonal, and is given for the λth hyperfine line of degeneracy D_λ by

$$-R_\lambda^{\rm HE}=[(N-2D_\lambda)/N]\omega_{\rm HE}\equiv f_\lambda^{-1}\omega_{\rm HE}. \tag{2.24}$$

The K matrix is also diagonal with $K_\lambda=\Delta\omega_\lambda$, and when the λth line is near resonance only $\bar{Z}_\lambda''$ will be appreciably different from zero, so the other transitions may be neglected. Now the vector $\mathbf{Q}'$ replaces $\mathbf{Q}$ and has elements $Q_\lambda'=D_\lambda d_\lambda q$, where $q=\hbar/NkT$,[29] and $d_\lambda=\frac{1}{2}\gamma eB_1$, where B_1 is the strength of the *rotating* microwave field. We then have

$$\bar{Z}_\lambda''=-R_\lambda^{-1}Q_\lambda'/[1+R_\lambda^{-2}\Delta\omega_\lambda^2+(-R_\lambda^{-1})S_{\lambda,\lambda}'], \tag{2.25}$$

where the saturation matrix element is given by $S_{\lambda,\lambda}=d_\lambda^2\Omega_\lambda D_\lambda$. Here Ω_λ is the saturation parameter for the λth (degenerate) transition. A method for calculating Ω_λ is discussed in Ref. 13, but it is rather complex, so only a few simple cases, which are inadequate for the experiments described here, have been solved. There is, however, a much simpler procedure, which yields more general results when certain conditions are fulfilled.

(1) All spin–flip relaxation transitions are either pure electron-spin (W_e) and/or pure nuclear-spin–flip (W_n) processes and/or exchange processes.

(2) The pure electron-spin–flip processes are equal for $+\rightarrow -$ and $-\rightarrow +$ transitions, and the pure nuclear-spin–flip processes are independent of M_s.

Then utilizing this procedure (which is developed in Appendix B) we obtain, when only $\omega_{\rm HE}$ and W_e are important;

$$\Omega_\lambda=(2/W_eD_\lambda)(1+D_\lambda b'')/(1+\tfrac{1}{2}Nb''), \tag{2.26}$$

where

$$b''=\omega_{\rm HE}/NW_e. \tag{2.26'}$$

A comparison of Eq. (2.25) with that of a simple saturated Lorentzian yields for an experimentally measured $T_{1,\lambda}$

$$T_{1,\lambda}=\tfrac{1}{4}(D_\lambda\Omega_\lambda). \tag{2.27}$$

These results are found to have a simple physical interpretation. Line broadening [Eq. (2.24)] is a lifetime-uncertainty effect given by the frequency with which an electron spin exchanges its original nuclear-spin environment for another that corresponds to a different resonance transition. This exchange frequency, by coupling the different possible resonant

[28] J. H. Freed, J. Chem. Phys. **43**, 2312 (1965).

[29] It should be noted that while the definition $q=\hbar/kT$, was given in the earlier papers,[10,13,28] all results of these papers are correct with $q=\hbar/NkT$.

transitions, allows a saturated transition to relax via lattice-induced electron-spin flips (W_e) occurring for the other hyperfine transitions. Thus, for $b''\gg 1$, Eqs. (2.26) and (2.27) give

$$T_{1,\lambda}(b''\to\infty)=(2D_\lambda/N)T_{1,\lambda}(b''=0), \quad (2.28)$$

where $T_{1,\lambda}$ is reduced from its value for $b''=0$ by the ratio of the degeneracy of the λth transition to the total number of transitions, including degeneracies.

III. EXPERIMENTAL METHODS

A. Materials

The KTCNE was supplied to us by R. E. Benson of E. I. Dupont de Nemours and Company. It was stored in a sealed bottle at 0°C. The dimethoxyethane (DME) and tetrahydrofuran (THF) were Eastman white label and were purified by usual methods.[30] Density and viscosity values for THF and DME were taken from the work of Swarc and co-workers.[31] The DTBN was synthesized by Bruce Kaplan using the method of Hoffman *et al.*[32a]

B. Preparation of Samples

The samples were prepared in a 15-mm-o.d. Pyrex calibrated sample tube containing a large storage sidearm, a 4-mm-o.d. quartz sidearm, and a 3-mm-o.d. Pyrex sidearm. The quartz sidearm was used for concentration measurements because the pitch standard sample was in a tube of the same diameter (cf. Sec. III.D). The Pyrex sidearm was used for variable-temperature measurements. This was because the temperature controller did not function well with a 4-mm-o.d. tube. The sample tube was calibrated by successively pipetting 10 1-ml aliquots of water into the calibration side of the tube and marking on the tube the bottom of the meniscus after each addition.

Before preparing the sample, the sample tube was washed with an ethanolic sodium hydroxide solution, rinsed with distilled water, and "flamed out" on the vacuum line.[33] These steps were taken to remove contaminating substances that might react with the radical. After flaming, the tube was allowed to cool and was then removed from the vacuum line. A weighed sample of KTCNE was placed in the tube, which was then immediately placed on the vacuum line and evacuated. This was done to protect the KTCNE from moisture and oxygen. The purified DME (or THF) was then distilled under high vacuum into the calibrated side of the sample tube. The sample was degassed to ensure complete removal of oxygen and then sealed from the line. Samples prepared in this manner were stable for months. The sample was diluted by allowing the desired fraction of the total solution to flow into the storage side of the sample tube; then the DME in this fraction was distilled back to the calibrated side. Distillation was easily accomplished by placing the calibrated side in a Dewar of LN_2.

It was noted that KTCNE did not dissolve as readily in THF as in DME. A great deal of shaking and heating of the sample tube with warm water were required for complete dissolution. Once dissolved, the $TCNE^-$ did not precipitate out of solution at temperatures as low as 203°K and at radical concentrations as high as 2.8×10^{-3} M. Although a careful study was not made, it appears that $TCNE^-$ decomposes more rapidly in THF than in DME. This decomposition is often first noted after a month or two, when a black substance precipitates out that cannot be returned to the solution. Over the period of time (about 2 weeks) that individual samples were used for experiments, however, no decomposition was noted.

C. Linewidth Measurements

All measurements were carried out on a Varian V4502-14 X-band ESR spectrometer system employing a 12-in. magnet. The temperature of the sample was controlled by a Varian V-4540 variable-temperature controller, and was measured using a copper–constantan thermocouple. It is estimated that the temperatures were known to ±2°C and controlled to ±1°C for the T/η studies and known and controlled to ±1°C for the studies at 15°C. Particular care was taken to insulate the magnet Hall probe and the body of the Varian V4535 cavity from chilled nitrogen issuing from the Dewar used in the temperature controller. If these precautions were not taken, wide variations in linewidth at a given temperature were sometimes noted. The magnetic field sweep was calibrated either with a Harvey Wells Model G-502 NMR precision gaussmeter or by an electrolytically generated sample of a durosemiquinone radical in DME (splitting 1.917 G[34]).

In different runs, various different field-modulation frequencies of 400 and 800 Hz, 6, 15, or 100 kHz were used. In general, the frequency was chosen to be low

[30] J. R. Bolton and G. K. Fraenkel, J. Chem. Phys. **40,** 3307 (1964).

[31] C. Carvajal, K. J. Tolle, J. Smid, and M. Szwarc, J. Am. Chem. Soc. **87,** 5548 (1965).

[32] A. K. Hoffman and A. T. Henderson, J. Am. Chem. Soc. **83,** 4671 (1961).

[33] The referee has pointed out that it is possible in this procedure for Na^+ ions to remain in the glass even after washing. These Na^+ ions could subsequently exchange with K^+ from the K^+TCNE^- solutions. P. Graceffa and T. R. Tuttle, Jr. [J. Chem. Phys. **50,** 1908 (1969)] discuss effects due to K^+ being picked up by anionic free-radical solutions. They suspect that K^+ adsorbed on glassware is brought into solution through ion exchange. In some of our later experiments (using 6-KHz field modulation and DME solvent), we did not use alkaline NaOH, but washed the sample tubes with distilled water, and dried them in an oven overnight at 180°. This was followed by baking with a bunsen flame while the tubes were under a vacuum <1 μ. Those solutions which overlapped in concentration with the original work, yielded the same widths and saturation parameters within experimental error.

[34] M. R. Das (unpublished results).

enough so as not to appreciably broaden the hyperfine lines.[35] In one case, however, the experiments with the 2.5×10^{-3} M DME solution utilizing 100-kHz modulation, small corrections[35] ranging from 2% to 7% were required for lines narrower than 200 mG. For the narrow line samples the X-band bridge was operated in the low power configuration. The incident power on the cavity ($\sim$0.05 mW) was kept low to avoid saturation effects. The resulting signal-to-noise ratio was about 20 to 1 at audio-modulation frequencies. The linewidths measured are probably good to ±3 or ±4 mG. The modulation amplitude in these experiments was kept at $\frac{1}{10}$ (or less) of the first-derivative linewidths, so no corrections needed to be applied to the experimental results for modulation amplitude broadening.

Care was taken to work within a range of exchange frequencies where there was negligible overlap of hyperfine lines. In the present work with $TCNE^-$ we have found this condition to be fulfilled for $\omega_{HE}/a<0.3$ in accordance with Plachy and Kivelson's results[6] with a simple three-line spectrum.

D. Concentration Measurements

All measurements of the free-radical concentration were carried out using a Varian V-4532 dual-sample cavity in a manner similar to that described by Hyde and Brown[36] except that double integrations were performed instead of the equivalent first moment integrations. A Varian 0.1% pitch in KCl sample (in a 4-mm-o.d. quartz tube) served as a convenient secondary standard of known spin concentration. The primary standard for spin concentration measurement was a freshly prepared sample of DTBN in hexane (see below). The first-derivative output of the spectrometer was integrated by a Philbrick U2-T integrator module with a Philbrick UPA-2 operational amplifier. The resulting absorption curves were then integrated with a planimeter. Typical determinations were carried out to a precision of $\pm5\%$ (error limits in this work represent the sample deviation).

The spin concentration of the pitch sample was determined in the EPR dual-sample cavity relative to a sample of DTBN in spectrophotometric-grade hexane. The DTBN solution was prepared and degassed in a sample tube which was equipped with a 4-mm-o.d. quartz sidearm for ESR measurements and a Pyrocell No. 6008 rectangular cell with a 1-mm light path for uv measurements. The concentration of DTBN was determined before and after the EPR measurements by uv at 2380 **B** ($\epsilon=2140$).[32] No decomposition of the DTBN sample took place during the ESR measurements. The spin concentration determined for the pitch sample was $4\pm0.28\times10^{15}$ spins/cm of sample. A second pitch sample calibrated relative to the first had $2.7\pm0.32\times10^{15}$ spins/cm of sample. (Varian Associates estimate $3\pm0.75\times10^{15}$ spins/cm of 0.1% pitch sample in a 4-mm-o.d. tube.)

To measure the temperature variation of spin concentration in THF solutions, a $TCNE^-$ sample of known spin concentration was placed in one section of the dual-sample cavity. This section was equipped with the temperature-controller assembly. The other section of the dual-sample cavity contained the 0.1% pitch spin concentration standard. The temperature of the $TCNE^-$ sample was varied and the integrated intensity of the resulting signal was compared with the integrated intensity of the pitch sample that remained at room temperature.

E. Saturation Measurements

The technique of continuous saturation was used to determine the relaxation times. Procedures and precautions outlined previously[35,37] have been observed. The following points should also be noted.

In all experiments the cavity was critically coupled. Q was determined using the relation

$$Q_0=2Q_L=(2\nu_0)/(\Delta\nu),$$

where Q_0 is the unloaded Q, Q_L the loaded Q, ν_0 the cavity resonance frequency, and $\Delta\nu$ the bandwidth of the cavity absorption dip. The bandwidth is defined as the frequency difference between the two points on the cavity absorption dip where the power reflection coefficient $\Gamma^2=\frac{1}{2}$. It was determined from an experimental plot of the reflection coefficient versus the klystron frequency.[35] We obtained $Q_0=4350$ for the DME solvent at 15°C. The incident and reflected power from the cavity was measured using a Hewlett–Packard 431B power meter employing an X-band thermistor mount. This mount was placed on a 20-dB coupler connected to the waveguide carrying microwave power to and from the cavity. The klystron frequency was measured using a Hewlett–Packard transfer oscillator.

The line shapes at high and low radical concentrations were checked by comparing the first-derivative line shape of an experimental line with the first-derivative line shape of a Lorentzian line having the same first-derivative peak-to-peak amplitude and linewidth as the experimental line. Figure 1 gives such a comparison for the center line of a $7\times10^{-4}M$ $TCNE^-$ sample. For a perfect Lorentzian line, the points would fall on the solid line in Fig. 1. Thus, it is seen that the experimental line is Lorentzian within experimental error to five first-derivative half-widths. No meaningful measurements on the experimental line could be made beyond this distance from the derivative zero. Similar measurements were made for a $1\times10^{-4}M$ solution of $TCNE^-$

[35] R. G. Kooser, W. V. Volland, and J. H. Freed, J. Chem. Phys. **50,** 5243 (1969).

[36] J. S. Hyde and H. W. Brown, J. Chem. Phys. **37,** 368 (1962).

[37] R. G. Kooser, Ph.D. thesis, Cornell University, Ithaca, N.Y., 1968.

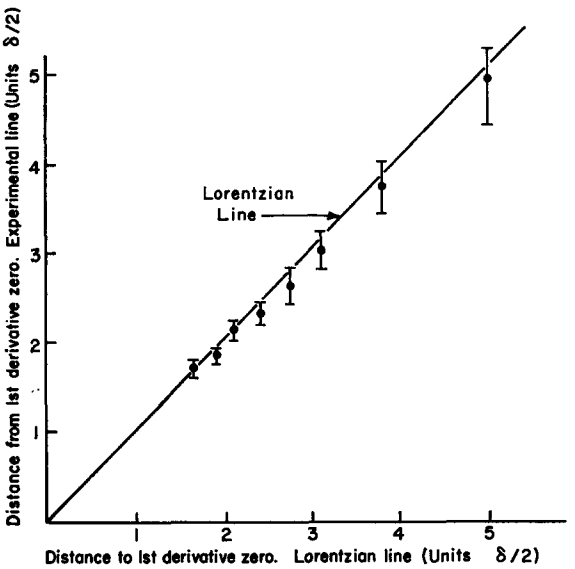

FIG. 1. Line-shape determination for the $\bar{M}=0$ line in the spectrum of a $7\times10^{-4}M$ solution of $TCNE^-$ in DME, $T=15°C$. The distance (in units of half the derivative width) of the experimental line is compared to the distance at which a Lorentzian line has the same relative amplitude.

in DME and for $1\times10^{-5}M$ (at 254°K) and $7.6\times10^{-4}M$ (at 241°K) solutions of $TCNE^-$ in THF. These lines were also Lorentzian within experimental error to five first-derivative half-widths from the derivative zero. Because the lines are Lorentzian, the following relationship applies[38]:

$$\delta^2=(4/3)(1/\gamma^2T_2^2)+(4/3)(T_1/T_2)B_1^2.$$

Here δ is the first-derivative linewidth, γ the gyromagnetic ratio, and B_1 the rf magnetic field.

The Varian V-4500 X-band bridge in the low-power configuration was used for all saturation runs. All relaxation times were corrected for the nonuniform microwave and modulating fields and for distortions of cavity modal pattern.[35]

IV. LINEWIDTH STUDIES

It follows from Eq. (2.24) that in the slow-exchange limit ω_{HE} is related to δ for a Lorentzian line by

$$\omega_{HE}=\tfrac{1}{2}\sqrt{3}f_{\bar{M}}\,|\,\gamma_e\,|\,[\delta_{\bar{M}}-\delta_{\bar{M}}(0)], \tag{4.1}$$

where the subscript $\bar{M}$ refers to the spectral index number of the line being considered,[14] and $\delta_{\bar{M}}(0)$ is the linewidth in the absence of exchange.

The second-order rate constant for an exchange process can be determined in two ways from our results. One method, which makes use of the linewidth measurements at different temperatures for a single sample, involves obtaining the linewidths $[\delta_{\bar{M}}-\delta_{\bar{M}}(0)]$ vs T/η. A plot of such data will be linear for the case of strong exchange, and the slope (for a line with spectral index number $\bar{M}$) will have the constant value $g_{\bar{M}}$. Since $\omega_{HE}=\tau_2^{-1}$ in the case of strong exchange, we have from Eq. (2.16) that

$$\tau_2^{-1}=f_{\bar{M}}\tfrac{1}{2}\sqrt{3}\,|\,\gamma_e\,|\,g_{\bar{M}}T/\eta, \tag{4.2}$$

and the second-order rate constant is given by $k\equiv(\tau_2C)^{-1}$, where C is the radical concentration. Also, for strong exchange, k may be obtained from the slope $h_{\bar{M}}$ of a linear plot of $[\delta_{\bar{M}}-\delta_{\bar{M}}(0)]$ vs concentration at constant temperature [or just $\delta_{\bar{M}}$ need be plotted when $\delta_{\bar{M}}(0)$ is independent of concentration]. That is

$$k=f_{\bar{M}}\tfrac{1}{2}\sqrt{3}\,|\,\gamma_e\,|\,h_{\bar{M}}. \tag{4.3}$$

The latter method is also applicable for weak exchange as well, but will yield

$$k'=\omega_{HE}/C=k[J^2\tau_1^2/(1+J^2\tau_1^2)].$$

A. DME Solutions

Figure 2(a) shows the actual derivative linewidth of the $\bar{M}=0$ line as a function of T/η for a $2.5\times10^{-3}M$ solution and for a $3\times10^{-5}M$ solution. One can obtain a good estimate of $[\delta_0-\delta_0(0)]$ for the $2.5\times10^{-3}M$ solution by subtracting these two linear results. Since $\delta_0(0)$ makes only a small and linear correction, we note that for the $2.5\times10^{-3}M$ solution, the good linear dependence (with positive slope) of the $\bar{M}=0$ linewidth with T/η indicates strong exchange. The portion of the linewidth for the $2.5\times10^{-3}M$ solution attributable to exchange was corrected for the effect of changes in solvent density on the radical concentration. This was done by multiplying $[\delta_{\bar{M}}-\delta(0)]$ at each temperature by the ratio ρ_0/ρ_T. Here ρ_0 is the solvent density at the temperature at which the concentration measurements were made, and ρ_T is the solvent density at the temperatures at which $[\delta_{\bar{M}}-\delta(0)]$ was determined. It should be noted that a correction of this type assumes that the linewidth is linear with the radical concentration, which is verified below. If electron–electron intermolecular dipolar interactions contributed appreciably to the measured linewidths in the concentrated sample, these linewidths should not be linear with T/η, because dipolar effects should be linear in η/T (see Appendix C). Also, when the experimental results are extrapolated to $T/\eta=0$, it is seen that the linewidth intercepts for the dilute and concentrated samples are the same, within experimental error, thus indicating that dipolar interactions make no experimentally significant contribution to the measured linewidths even at the higher concentration. This observation is supported by approximate calculations of dipolar effects (see Appendix C).

Table I contains the least-squares slopes and intercepts of the linewidth-vs-T/η plots for the various lines

[38] J. W. H. Schreurs and G. K. Fraenkel, J. Chem. Phys. **34**, 756 (1961).

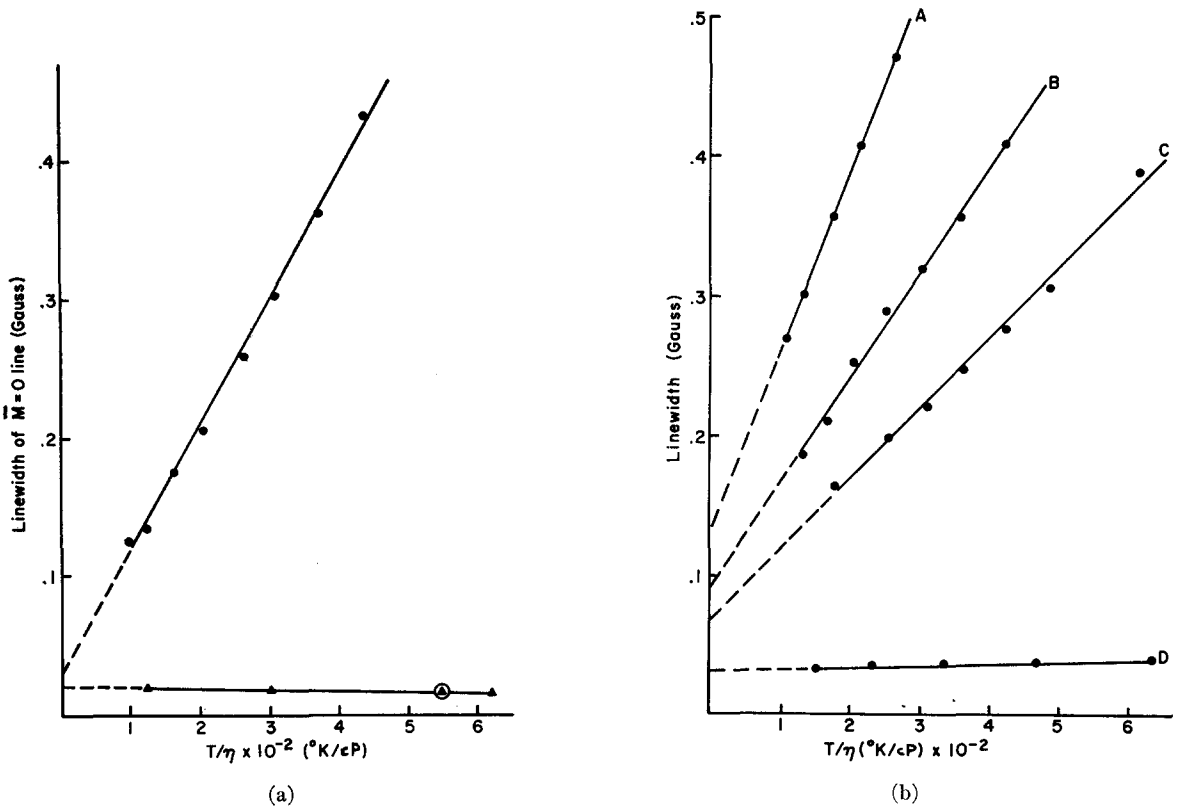

FIG. 2. Width of the $\bar{M}=0$ line vs T/η for $TCNE^-$ samples. (a) ●, DME solvent, $2.5\times10^{-3}M$; ▲, $3\times10^{-5}M$ in $TCNE^-$. (b) A, THF solvent, $2.8\times10^{-3}M$; B, $1.3\times10^{-3}M$; C, $7.6\times10^{-4}M$; D, $1\times10^{-5}M$ in $TCNE^-$.

studied. Because of possible line-shape distortion by ^{13}C splittings, the $\bar{M}=\pm3$ and $\bar{M}=\pm4$ lines were not studied.[14] All hyperfine lines for the dilute sample gave the same linewidths within ±2 mG (cf. Appendix D), and the results for $\bar{M}=0$ are given in the table. The value of ω_{HE} according to Eqs. (4.1)–(4.2) requires subtracting the value of the slope $g_{\bar{M}}$ of the low concentration study from that of the higher concentration results and in this case the subtraction term is not significant within experimental error. It is noted that the statistical effect leading to variations in width of lines with different values of $|\bar{M}|$ as predicted by Eq. (2.24) is evident in the slopes of the various hyperfine lines in Table I, and there is good agreement within experimental error. The individual results at each temperature were also compared for this statistical effect. The agreement between the predicted and observed values was good for a comparison between the $\bar{M}=+1$, $+2$ and 0 lines but not as good for the $\bar{M}=-1$, and -2 lines. This appears to be reflected in

TABLE I. Least-squares slope and intercept for fit of exchange data for TCNE:DME to $\delta=g(T/\eta)+\delta(T/\eta=0)$.

C (moles/liter)	$\bar{M}$	$\delta(T/\eta=0)$ (G)[a]	g(G·cP/°K)$\times10^4$ [b]	Predicted slope (G·cP[c]/°K)$\times10^4$
2.5×10^{-3}	2	0.026±0.004	10.2±0.2	10.3±0.3
2.5×10^{-3}	1	0.026±0.009	9.4±0.3	9.4±0.3
2.5×10^{-3}	0	0.027±0.008	9.0±0.3	...
2.5×10^{-3}	−1	0.024±0.004	9.4±0.2	9.4±0.3
2.5×10^{-3}	−2	0.021±0.004	10.2±0.2	10.3±0.3
3×10^{-5} [d]	0	0.021±0.001	−0.08±0.001	

[a] Errors represent standard deviation in the least-squares intercept.
[b] Errors represent standard deviation in the least-squares slope.
[c] The predicted slope is determined by applying theoretical statistical factor to the slope of the $\bar{M}=0$ line.
[d] All hyperfine lines gave the same linewidths within ±2 mG.

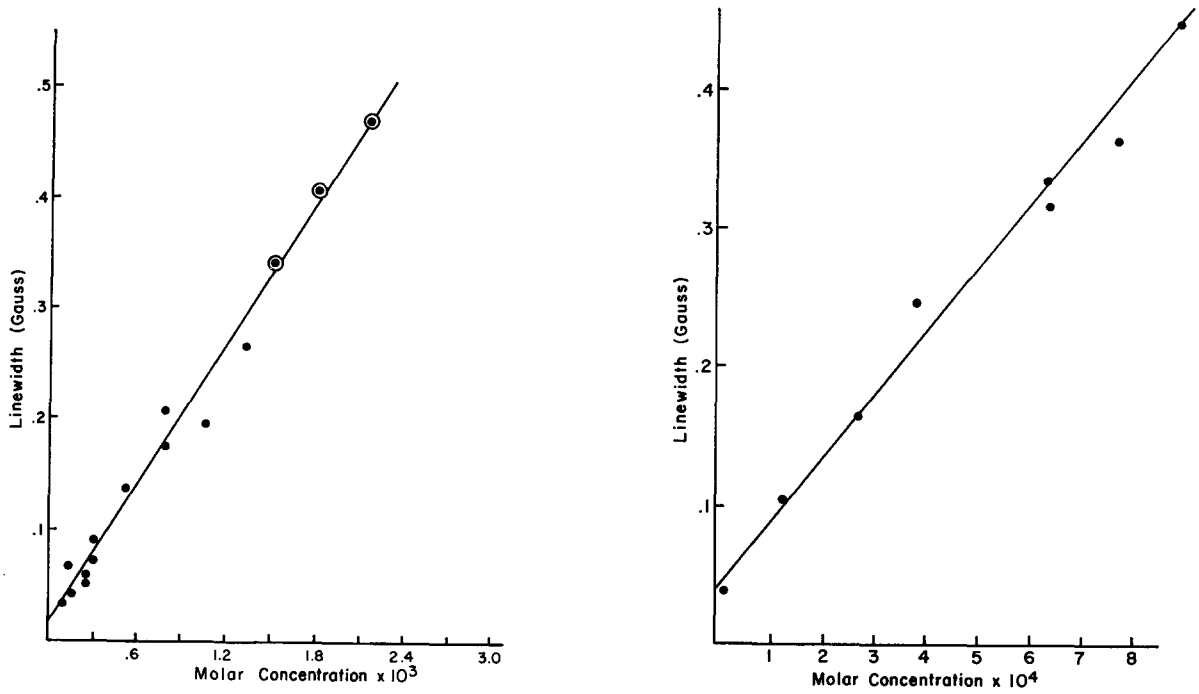

FIG. 3. Width of the $\bar{M}=0$ line vs concentration for $TCNE^-$ samples in (a) DME ($T=288°K$) and (b) THF ($T=296°K$). All points circled were obtained using 100-kHz modulation; all other points using audio-frequency modulation.

the variation in values for the intercepts of the different lines as summarized in Table I that is nevertheless within experimental error. When the widths at the different T's were adjusted to give the same intercept for all lines (which is permissible within experimental error), while retaining the same slopes, much better agreement was obtained. Both the original and adjusted results are summarized in Table II, where $F_{\bar{M},\bar{M}}=f_{\bar{M}'}/f_{\bar{M}}$. The adjusted results are found to be esentially independent of choice of the common value of $\delta(0)$ within 21–27 mG. Note that besides experimental errors, any variation in widths arising from concentration-independent relaxation effects (see Appendix D) should be cancelled out by this procedure.

Figure 3(a) shows the linear relation between linewidth and concentration for $\bar{M}=0$.[39] The point circled in Fig. 2(a) was obtained by extrapolation to zero concentration in Fig. 3(a). This point is very close to that expected for a $3\times10^{-5}M$ radical solution at 15°C, and verifies that exchange makes a very small contribution to the dilute solution linewidths. At 15°C, the data in Figs. 2(a) and 3(a) yield values for k of $4.1\pm0.6\times10^9M^{-1}\cdot\text{sec.}^{-1}$ and $4.3\times10^9M^{-1}\cdot\text{sec.}^{-1}$, respectively, or an excellent agreement. No error limits are placed on the value from Fig. 3(a) because the error incurred by diluting the original $3\times10^{-3}M$ sample is not accurately known. When the points in Fig. 2(a) are corrected for estimates of dipolar interactions (see Appendix C) between radicals, k becomes $4.2\times10^9M^{-1}\cdot\text{sec.}^{-1}$, a negligible change within experimental error.

[39] These experiments were carried out several months after the experiments summarized in Fig. 2(a). During this period the sensitivity of the audio-frequency unit was improved.

B. THF Solutions

Figure 2(b) shows the width of the $\bar{M}=0$ line vs T/η for several solutions of $TCNE^-$ in THF. These results have been corrected for the effect of changes in solvent density on the radical concentration, as described in Sec. IV. The plots are linear within experimental error for a given concentration. In this respect no difference is noted between the solvents THF and DME. An important difference is, however, reflected in the extrapolated linewidth intercepts. For the $TCNE^-$:DME solution the linewidth intercept does not depend on concentration [see Fig. 2(a)], but for the TCNE:THF solutions there is a definite increase in the extrapolated intercept with increasing radical concentration. The least-squares slopes and intercepts for the lines in Fig. 2(b) are summarized in Table III. This table also gives the values of k obtained with Eq. (4.2). Note that in Table III, the first three samples were prepared by diluting a $1.3\times10^{-3}M$ solution. All hyperfine lines for the $1\times10^{-5}M$ solution gave the same linewidth within ±2 mG as in the $TCNE^-$:DME system, and these results were used as our estimate of $\delta(0)$.

Figure 3(b) shows the dependence of the width of the $\bar{M}=0$ line on concentration at 23°C. This plot is again linear within experimental error, and it yields a value of $9\pm1\times10^9 M^{-1}\cdot$sec.$^{-1}$ for k. Using this result, a value for k at 15°C can be estimated to be $8\pm1\times10^9 M^{-1}\cdot$sec.$^{-1}$ Also the existence of the statistical factor $f_{\bar{M}}$ demonstrated for the TCNE$^-$:DME system was verified within experimental error for the TCNE$^-$:THF system as well. The rate constant k from Fig. 3(b) and those in Table III differ somewhat; however, the difference is within experimental error. The value of k determined for the $2.8\times10^{-3}M$ sample is somewhat less than that determined for the other samples (see Table III), but is believed to be a less accurate result.

TABLE II. Experimental values of $F_{\bar{M},\bar{M}'}$ for TCNE:DME.

Predicted / T(°K)	$F_{-1,0}$[a]	$F_{1,0}$[a]	$F_{-2,0}$[b]	$F_{2,0}$[b]
	1.048	1.048	1.145	1.145
A. Uncorrected results				
203	1.009	1.038	1.077	1.115
211	1.008	1.018	1.071	0.140
223	1.012	1.032	1.097	1.143
233	1.038	1.043	1.113	1.108
243	1.025	1.034	1.092	1.118
252	1.035	1.043	1.113	1.121
262	1.035	1.038	1.109	1.120
272	1.041	1.041	1.116	1.138
B. Corrected results				
203	1.041	1.052	1.144	1.134
211	1.037	1.028	1.131	1.159
223	1.034	1.041	1.142	1.156
233	1.056	1.050	1.150	1.170
243	1.039	1.039	1.121	1.125
252	1.047	1.047	1.138	1.127
262	1.045	1.042	1.128	1.125
272	1.049	1.044	1.133	1.142

[a] Standard deviation ±0.012.
[b] Standard deviation ±0.014.

Figure 4 is a plot of linewidth intercepts versus relative radical concentration. The points in this plot were taken from Table III, using only the data for the 1.3×10^{-3} M solutions and its diluted forms. It is seen that the linewidth intercept increases in a linear manner with concentration. This conclusion does not depend on an accurate absolute measurement of spin concentration; it depends only on the accurate dilution of the sample, which is not difficult to perform (see Sec. III.B). These results for the $\bar{M}=0$ exchange linewidth of TCNE$^-$ in THF can be represented by the expression

$$\delta=A(T/\eta)C+BC+\delta(0). \tag{4.4}$$

The value for B(48 GM^{-1} or 7.3×10^8sec$^{-1}\cdot M^{-1}$ in terms of a rate constant) is determined from Fig. 4, and the value for A (0.570 G$\cdot$cP°K$^{-1}\cdot M^{-1}$) is determined from Fig. 2(b) (using only the data for the $1.3\times10^{-3}M$ solution and its diluted forms). The B term in the above expression for δ is probably due to some line-broadening process other than exchange. We are not able to estimate its temperature dependence, if any, from our data. If the contribution to the linewidth from the B term is subtracted from the slope of the line in Fig. 3(b), k becomes $7.2\pm1\times10^9 M^{-1}\cdot$sec.$^{-1}$ at 15·C (and $8.2\pm1\times10^9 M^{-1}\cdot$sec.$^{-1}$ at 23°C.), which is in excellent agreement with the results in Table III, as might have been anticipated from the studies of TCNE$^-$ in DME.

TABLE III. Least-squares slope and intercepts for fit of $\bar{M}=0$ linewidth (for TCNE$^-$ in THF) to $\delta=g(T/\eta)+\delta(T/\eta=0)$.[a]

Concentration (moles/liter)	$\delta(T/\eta=0)$ (G)	g(G·cP/°K) $\times10^8$	$k(M^{-1}\cdot$sec$^{-1})$
1×10^{-5} [b]	0.031±0.001	0.012±0.002	···
7.6×10^{-4} [b]	0.066±0.007	0.50±0.02	$6.9\pm1\times10^8$
1.3×10^{-3} [b]	0.093±0.007	0.74±0.02	$6.9\pm1\times10^9$
2.8×10^{-3}	0.132±0.006	1.28±0.03	$5.2\pm0.8\times10^9$

[a] Error limits represent standard deviation in least-squares fit to the data.
[b] All of these samples were prepared by dilution of a $1.3\times10^{-3}M$ TCNE$^-$ in THF solution.

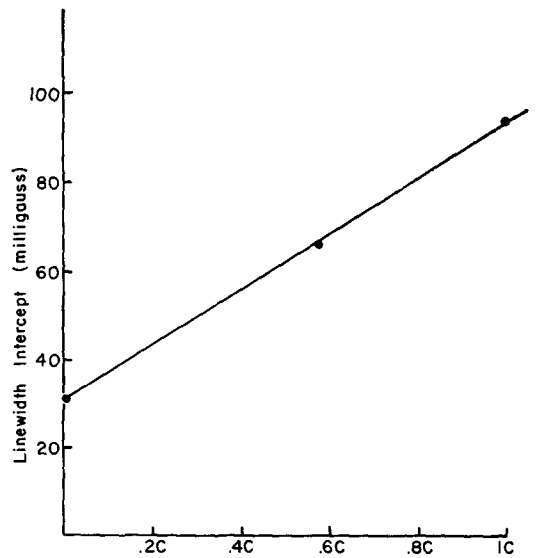

FIG. 4. Linewidth intercept [as determined from Fig. 3(b)] vs radical concentration. The nominal value for C is $1.3\times10^{-3}M$.

TABLE IV. Purity of the KTCNE used in linewidth studies.

Concentration (moles/liter)[a]	Solvent	Purity[b]
$2.4\pm0.28\times10^{-3}$	DME	100%
$2.5\pm0.30\times10^{-3}$	DME	99%
$3.0\pm0.36\times10^{-3}$	DME	92%
$2.8\pm0.34\times10^{-3}$	THF	74%
$1.3\pm0.16\times10^{-3}$	THF	71%

[a] Determined from dual sample cavity measurements at 295°K.
[b] The purity was determined by comparing the sample concentration from the dual sample cavity measurements with the sample concentration calculated on the basis of the weight of $KTCNE^-$ and the volume of solvent.

C. Radical Concentration Measurements

The measurements of the absolute radical concentrations in $TCNE^-$:THF solutions indicated that the $TCNE^-$ was about 71%–74% pure. Similar measurements in DME indicated the $TCNE^-$ purity was between 92% and 100%. The results of all concentration measurements where the $TCNE^-$ purity was determined are summarized in Table IV.

Although the above measurements of purity are almost within experimental error,[40] it seems strange that all the low-purity values are closely grouped and are obtained for THF solutions while all the high-purity values are closely grouped and are obtained for DME solutions. It might be argued that the $TCNE^-$ reacts with impurities present in the THF and this decreases the radical concentration. However, both the DME and THF were purified in the same manner (see Sec. III.B), and therefore it is very unlikely that there is an impurity capable of destroying the $TCNE^-$ radical in the THF that is not also present in the DME. As noted in Sec. III, KTCNE did not dissolve easily in THF. The sample tube had to be heated with warm tap water to completely dissolve the KTCNE. It cannot be entirely ruled out that this slight heating caused some decomposition of the $TCNE^-$.

In another study the relative concentration of $TCNE^-$ radicals in THF was measured as a function of temperature. The results (see Table V) were corrected for Curie law paramagnetism[41] and changes in solvent density. The Curie law correction was necessary because the standard sample was maintained at room temperature while the temperature of the $TCNE^-$:THF sample was varied. Within experimental error the results in Table V show no radical concentration variation with temperature. However, the experimental error in Table V is quite large and it is possible that small (5%–10%) changes in radical concentration could be taking place in solution.

D. Exchange in DME and THF Solutions of DTBN

The results of the present study of spin exchange between DTBN radicals in DME and in THF are summarized Figs. 5. These results have been corrected for changes in radical concentration due to density changes in the manner already described. Figure 5(a) shows the width of the $\bar{M}=0$ line vs T/η for a $2.9\times10^{-5}M$ solution of DTBN in DME. For values of T/η greater than 3×10^2 °K/cP ($T=252$°K), the linewidth increases linearly with increasing values of T/η, which is probably due to spin–rotational relaxation.[6] In the region below $T/\eta=3\times10^2$ °K/cP, the linewidth does not change with T/η, probably because of the effects of the proton extra-hyperfine lines, which arise from the 18 equivalent *t*-butyl protons having a measured splitting constant of about 0.1 G. That is, the linewidth is now determined by an envelope of these proton hyperfine lines. As these proton hyperfine lines broaden with increasing T/η a point is reached (at about 3×10^2 °K/cP) where they coalesce into a single line which then broadens. The results for THF are very similar to those for DME and are therefore not given.[42]

The width dependence of the $\bar{M}=0$ line on T/η is given in Fig. 5(b) for $4\times10^{-3}M$ DTBN in DME and in THF. These results have already been corrected for spin–rotational contributions by subtracting the T/η-dependent portion of the low concentration widths.[6] Therefore, the increase in linewidth with increasing T/η should be due to spin exchange only. However, in the region where the linewidth is less than 1 G, it is still dependent upon the partially exchange-narrowed proton extra-hyperfine structure, so only linewidths greater than 1 G were used to determine the exchange rates. Also, all experiments were carried out

TABLE V. $TCNE^-$ concentration in THF as a function of temperature.

$TCNE^-$ concentration	T(°K)
2.6×10^{-3} [a]	254
$2.68\pm0.19\times10^{-3}$	244
$2.76\pm0.19\times10^{-3}$	235
$2.78\pm0.19\times10^{-3}$	222
$2.57\pm0.18\times10^{-3}$	207

[a] All concentrations were determined with respect to a nominal radical concentration of $2.6\times10^{-3}M$ at 254°K.

[40] The sources of error in the purity determinations are a standard deviation in absolute radical concentration measurements plus a small undetermined error in measuring the weight of KTCNE delivered to the sample tube and in the volume of the solvent added to the KTCNE.
[41] G. E. Pake, *Paramagnetic Resonance* (W. A. Benjamin, Inc., New York, 1962).
[42] It may be added that Plachy and Kivelson in their study of the DTBN radical in pentane[6] observed, for very dilute samples, only the region where the linewidth increased with T/η.

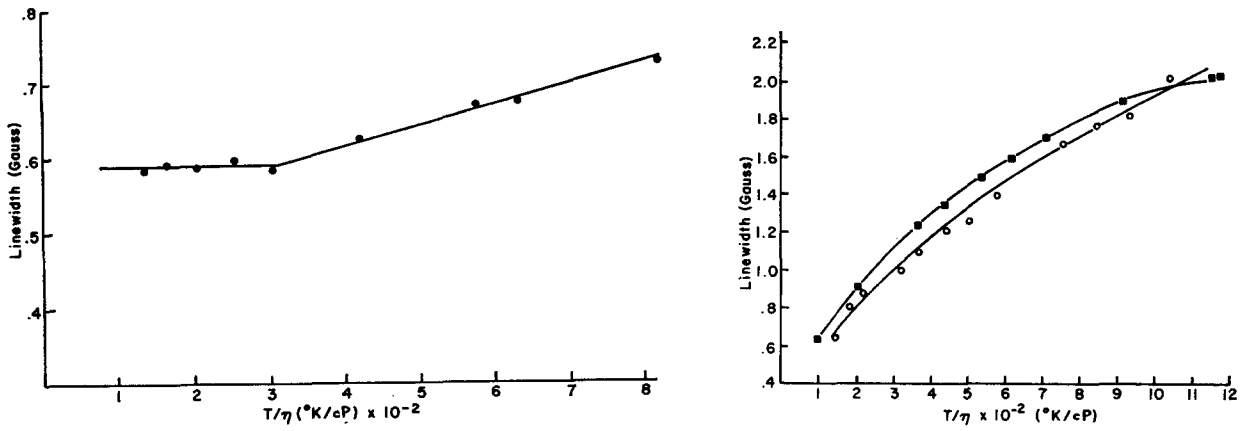

(a) (b)

FIG. 5. Width of the $\bar{M}=0$ line vs T/η for solutions of DTBN in DME and THF. (a) $2.9\times10^{-5}M$ in DME (nearly identical results in THF). (b) ○, $4\times10^{-3}M$ in THF; ■, $4\times10^{-3}M$ in DME, the spin–rotational contribution has been subtracted out.

for widths where there was negligible overlap of nitrogen hyperfine lines.[6,43]

Plachy and Kivelson have carefully studied DTBN spin exchange in pentane. Their results may be reinterpreted in terms of the continuum model [cf. Eqs. (2.16) and (2.17)] to yield a value of $k'=1.46\times10^{10}M^{-1}\cdot\text{sec}^{-1}$ at 25°C., where $k'/k=(J\tau_1)^2/(1+J^2\tau_1^2)=0.8$. If, however, their data are analyzed in the T/η region (0.5–2.2×10^5 °K·P) in which the corrected widths are linear in T/η, and we assume $k'/k=1.0$, or strong exchange, then from Eq. (4.2) we can estimate a value for $k'=k=1.5\times10^{10}M^{-1}\cdot\text{sec}^{-1}$ at 25°C, which agrees well with the sounder analysis, and, in fact, agrees well with the value of $1.45\times10^{10}M^{-1}\cdot\text{sec}^{-1}$ calculated from Eq. (2.16a) for strong exchange. Thus we expect that a reasonable estimate of k' may be obtained from our results of DTBN in Fig. 5(b), where the data are not quite linear, by utilizing a reasonable average slope in Eq. (4.2) and setting $k'=k$. The results for k we obtain in this manner are $6.4\times10^9M^{-1}\cdot\text{sec}^{-1}$ at 25°C in DME and $5.8\times10^9M^{-1}\cdot\text{sec}^{-1}$ at 25°C in THF, their difference being within the error of our simplified analysis.

Studies of DTBN spin exchange have also been carried out in water and are given elsewhere (Part II of series).

V. SATURATION STUDIES

The longitudinal relaxation time $T_{1,\bar{M}}$ has been determined as a function of concentration for three hyperfine lines ($\bar{M}=0,-1,-2$) in the $TCNE^-$:DME system. The results are displayed in Fig. 6. The expected decrease of T_1 toward an asymptotic limit is clearly evident in all cases. Included are "theoretical" curves obtained using Eqs. (2.26) and (2.27), for which it was necessary to determine b'' at the different concentrations. This was possible by utilizing the linear linewidth-vs-concentration fit of Fig. 3(a) and assuming $W_e=[2T_{1,\bar{M}}(0)]^{-1}$. That is

$$b''=(\sqrt{3}\,|\,\gamma_e\,|\,f_{\bar{M}}/N)\,T_1(0)[\delta_{\bar{M}}-\delta_{\bar{M}}(0)] \quad (5.1)$$

for each concentration.

In order to make a quantitative comparison between the theoretical and experimental results, it is necessary to determine the value of $T_{1,\bar{M}}(0)$ reasonably accurately. This requires an accurate saturation measurement at very low concentrations ($\sim10^{-5}M$), which is very difficult because one must determine small linewidth changes in very narrow lines with a low signal-to-noise factor. Also, there are problems of accurately determining such low radical concentration. Thus, most of the experiments were performed utilizing concentrations of $10^{-4}M$, and greater. (The scatter in the T_1 data at about $10^{-4}M$ is probably due to low signal-to-noise factors). However, it was later found that by working with 6-kHz field modulation (instead of 0.8 kHz utilized in the original work) the signal to noise was appreciably improved, yet the field-modulation frequency was still small enough to avoid any serious errors in the measurement of T_1 and T_2.[35]

Several low concentration studies were made for the $M=0$ line as indicated in Fig. 6(a). We note that while a value of $T_1(0)=6.0\times10^{-6}$ sec appears to give asymptotically better agreement for the $\bar{M}=0$ line, the value of $T_1(0)=7.0\times10^{-6}$ sec agrees well with the lower concentration $\bar{M}=0$ results and with the results on the $\bar{M}=-1$ and -2 lines.

It is possible to make a linear least-squares fit to the

[43] The value for a, the nitrogen hyperfine splitting constant, is 15.4 G in pentane,[6] 15.5±0.2 G in THF, and 15.2±0.18 G in DME. (The values for a in THF and in DME were determined in the course of the linewidth measurements.)

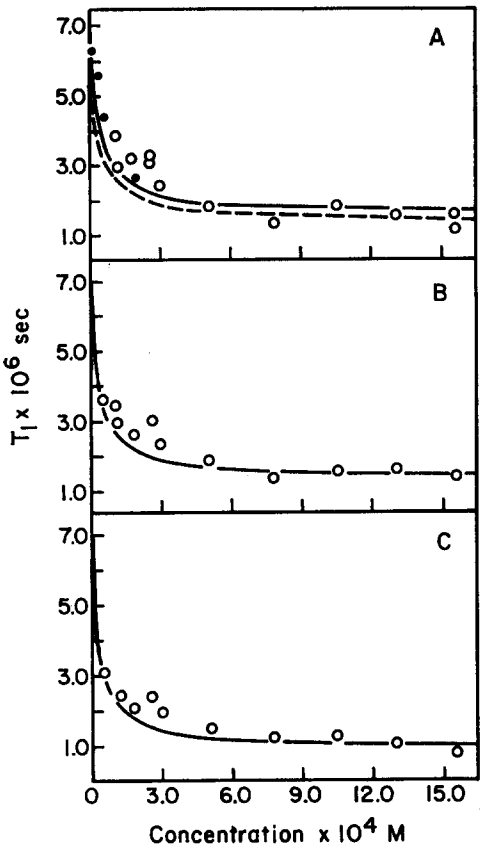

FIG. 6. T_1 as a function of concentration for $TCNE^-$ in DME at 15°C. The theoretical curves were determined using Eqs. (2.26), (2.27), and (5.1) with $T_1(0)=7.0\times10^{-6}$ sec (solid lines) and $T_1(0)=6.0\times10^{-6}$ sec (dashed line); (A), $\bar{M}=0$; (B), $\bar{M}=-1$; (C), $\bar{M}=-2$. The dark points correspond to 6-kHz field modulation, all others using low-frequency modulation.

data by rearranging Eqs. (2.26) and (2.27) to give

$$[1-T_{1,\bar{M}}/T_1(0)]^{-1}=m_{\bar{M}}b''^{-1}+a_{\bar{M}}, \qquad (5.2)$$

where the slope $m_{\bar{M}}=2f_{\bar{M}}/N$, and the intercept $a_{\bar{M}}=f_{\bar{M}}$. It is possible, then, for different estimated value of $T_1(0)$ [which also affects the value of b'' via Eq. (5.1) at each concentration] to look for the best least-squares fit according to Eq. (5.2). This was done for the $\bar{M}=0$ line [see Fig. 7(a)] and the results appear in Table VI. The best fit to both m and a appears to be for $T_1(0)\sim6.5$–7.0×10^{-6}sec, and in this range gives rather good agreement with the theoretical slope and intercept. However, one is struck by the extreme sensitivity of the experimentally determined slope upon the choice of $T_1(0)$. Thus, a 7% decrease in $T_1(0)$ yields a 50% increase in m. This is because the slope is largely determined by the low concentration measurements, and this region is where $T_{1,\bar{M}}/T_1(0)$ on the lhs of Eq. (5.2) differs only slightly from unity, so it is subject to significant variation from small changes in the choice of $T_1(0)$. (Also, the other sources of error for low concentration work, which have already been noted, become more critical.) Table VI and Figs. 7(b) and 7(c) also give the results for the $\bar{M}=-1$ and -2 lines assuming $T_1(0)=7.0\times10^{-6}$sec, and again the agreement is reasonably good, despite the absence of very low concentration points.

Besides the extreme sensitivity of the experimentally determined slope to the choice of $T_1(0)$ relative to the other T_1 values, there are other significant sources of error. First, are the possible systematic errors in the set of T_1 measurements from such sources as (1) the cavity-Q determination (estimated error of 15%), (2) the estimate of the geometric field distribution factor by the perturbed sphere method, and (3) the correction for variation of microwave and field-modulation amplitudes across the sample as discussed elsewhere.[35] We thus estimate an error of about 20%–30% in accuracy of T_1 measurements from these sources. This error will affect the determination of the slope of Eq. (5.2) via the dependence of b'' on $T_1(0)$ [see Eq. (5.1)] but will not affect the intercept. Also, errors in determining $\delta_{\bar{M}}(0)$ relative to the other $\delta_{\bar{M}}$ values will lead to significant errors in values of b'' for the low concentration samples where $\delta_{\bar{M}}-\delta_{\bar{M}}(0)$ is a small quantity. This source of error would most seriously affect the slope determination. Finally, we note that Eqs. (2.26), (2.27), and (5.2) are based on the assumption that all other nuclear-spin–flip processes are negligible. An outcome of our careful work at 6 kHz, was to show that this assumption is not entirely correct and this matter is more fully explored in Appendix D, where it is shown that the agreement with the experimentally determined intercept a can be improved by introducing corrections

TABLE VI. Least-squares fit for b''^{-1} vs $[1-T_{1,\bar{M}}/T_1(0)]^{-1}$ [a] for TCNE in DME.

$\bar{M}$	$T_1(0)$ $\times10^{-6}$ sec	Slope—$m\times10^2$	Intercept—a	Mean percent error
0	6.0	5.0±0.3	1.10±0.20	11.9
	6.5	2.40±0.16	1.40±0.10	7.2
	7.0	1.64±0.14	1.43±0.08	7.35
	7.5	1.27±0.13	1.41±0.07	7.85
	8.0	1.05±0.13	1.39±0.06	8.25
	Theoretical	1.61	1.31	···
−1	7.0	2.2±0.4	1.31±0.06	11.4[b]
	Theoretical	1.54	1.25	···
−2	7.0	1.4±0.2	1.21±0.04	8.8[b]
	Theoretical	1.41	1.14	···

[a] Errors represent the sample deviation. The mean percent error is the mean of the percent errors in m and a.

[b] Fewer experimental points taken for $\bar{M}=-1$ and -2 lines than for the $M=0$ line.

for small, but not negligible, electron–nuclear dipolar (END) interactions.

VI. DISCUSSION AND CONCLUSIONS

A. Linewidth Studies

A general feature of this work has been the good agreement between the values of k obtained from concentration and T/η studies. This is a good confirmation of the fact that strong exchange dominates the widths of the higher concentration solutions and also of the fact that other effects, such as dipolar interactions, are rather unimportant. It was also possible to obtain a good quantitative agreement for the statistical variation of the exchange contribution to the different hyperfine lines.

A summary of the measured values of k in this work appears in Table VII. In general, there is very good agreement with the theoretical prediction given by Eqs. (2.16a) and (2.17), where $f\cong 1$ (i.e., neglect of effects of charge) and $d\cong 2a$ (i.e., the minimum distance of approach). An obvious conclusion which may be drawn is that the effect of charge in the $TCNE^-$ spin exchange is relatively unimportant. However, an estimate of f for single like-charged radicals under conditions of our experiments is

$$f=\frac{70/d}{e^{70/d}-1},$$

which will be much less than unity unless $d>70$ Å.

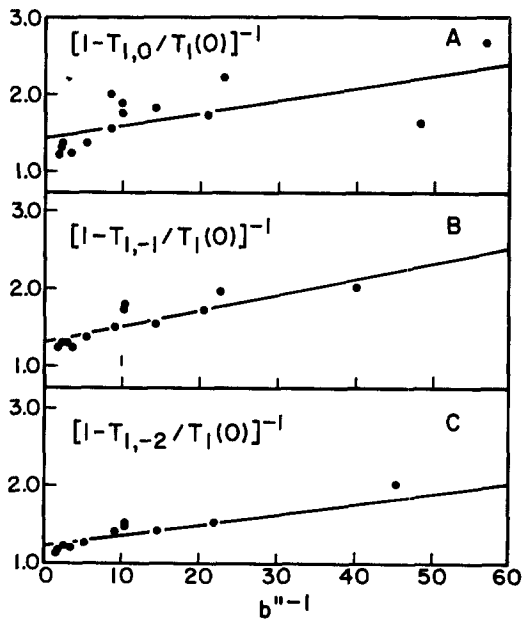

FIG. 7. Linear least-squares fit for $[1-T_{1,\tilde{M}}/T_1(0)]^{-1}$ vs b''^{-1} for $TCNE^-$ in DME at 15°C. $T_1(0)=7\times10^{-6}$ sec and b'' from Eq. (5.1). (A), $\tilde{M}=0$, $T_{2,0}(0)=3.97\times10^{-6}$ sec; (B), $\tilde{M}=-1$, $T_{2,-1}(0)=3.80\times10^{-6}$ sec; (C), $\tilde{M}=-2$, $T_{2,-2}(0)=3.34\times10^{-6}$ sec.

TABLE VII. A summary of spin-exchange rate constants k in DME and THF at 15°C.

Radical	Solvent	$k(M^{-1}\cdot\text{sec}^{-1})$ [a] Experimental	Theoretical
$TCNE^-$	DME	$4.1\pm0.6\times10^9$	6.4×10^9
$TCNE^-$	THF	$6.9\pm1\times10^9$	6.3×10^9
DTBN	DME	5.5×10^9 [b]	6.4×10^9
DTBN	THF	5.0×10^9 [b]	6.3×10^9

[a] The theoretical rate constant at 15°C [calculated on the basis of Eqs. (2.16a) and (2.17), assuming $f=1$ and $d=2a$].

[b] These rate constants are from the linewidth-vs-T/η data, assuming $k=k'$.

Since we would not expect J to be very significant beyond about 10 Å, it seems reasonable to assume that the effective charge on the radicals is significantly less than unity.[44] This is most likely a result of ion pairing, which is expected for these systems, although no direct evidence has as yet been found.[45,46] In principle, it would be possible to estimate an "effective" charge, if certain important details were better understood. These would include (1) the dependence of J on d, so that one could define a maximum value of d, for which strong exchange [i.e. $(J\tau_1)^2\gg1$][47] would still hold; as well as (2) the removal of the arbitrary two-jump theoretical model employed in Sec. II, in recognition of a continuum of J values. Also important would be a knowledge of steric factors, such as the effect on J of the relative orientation of the interacting radicals. If we naively neglect these and other considerations, then for the TCNE–DME result, if $d\sim2a\sim6$ Å, one obtains $Z_{\text{eff}}\sim\frac{1}{4}$, while for TCNE–THF $Z_{\text{eff}}\sim0$.

This points to a second observation, namely, there appears to be a significant difference between the measured values of k for TCNE in the two solvents although no such difference is predicted from Eqs. (2.16a) and (2.17). Furthermore, any such effect is less marked for DTBN, where any differences in k can be ascribed to experimental error. The direction of this trend is for more extensive (or stronger) ion-pair formation in THF as compared to DME, which is consistent with what is known about these sol-

[44] Similar conclusions appear to apply to the work discussed in Refs. 3 and 5, except that certain numerical factors are not entirely clear and in Ref. 3 no T/η-dependent studies are given to confirm that strong exchange was actually occurring.

[45] M. C. R. Symons, J. Phys. Chem. **71**, 172 (1967).

[46] We have found that in the $TCNE^-$/THF system the nitrogen hyperfine coupling constant does not change between 274°K and 215°K within five parts in 1000 or within the experimental error of seven parts in 1000. Often ion pairing leads to temperature variations of hyperfine couplings.

[47] It might be noted that even for strong exchange ω_{HE} may not be simply T/η dependent when charge effects are important, since f is a function of T through its dependence on $u\propto(\epsilon T)^{-1}$ (see Sec. II). However, in these solvents, the strong temperature dependence of $\epsilon=1.495+2659/T$ for THF[31] would tend to partially cancel out any effect on f.

vents[31,48–50] (viz., DME is the better solvating agent). However, there are two other anomalous observations with respect to the TCNE–THF study which were not observed in the DTBN work: (1) an apparent second linewidth effect dependent on concentration (cf. Figs. 14 and 16), and (2) an apparently lower purity for TCNE in THF as compared to DME. These observations would be reasonably consistent with a reaction in the THF solution, which at equilibrium tends to reduce the radical concentration, e.g., a disproportionation,

$$2K^+TCNE^- \rightleftharpoons TCNE + K_2^+TCNE^{2-}, \quad (6.1)$$

or a dimerization to form a diamagnetic product;

$$K^+TCNE^- + K^+TCNE^- \rightleftharpoons K_2^+TCNE^-_2. \quad (6.2)$$

The latter is strongly suggested by the observations that (1) the polycrystalline K^+TCNE^- exists almost completely in the singlet state with an associated triplet state for which $J=0.26$ eV[15]; (2) the related tetracyanoquinodimethane anion radical exhibits dimerization in aqueous solution.[51] In either case there could be a concentration-dependent width that is proportional to the forward rate constant, and an apparent reduction in purity that is dependent on the equilibrium constant.[52,53]

The observation that either equilibrium would lie more to the right in THF solution is consistent with other studies for both proposed types of mechanisms. Thus Hirota and Weissman in a study of the sodium fluorenone dimer,[54] which exists primarily in the triplet form, found a greater dissociation constant in DME than in THF solvent. Also, the nature of the equilibrium was found to have many similarities compared with simple ion-pair dissociation, including a small negative $\Delta H°$, but large negative $\Delta S°$ [these signs apply to the reverse reaction to Eq. (6.2)]. Similar statements may be made for studies by Garst and co-workers on the extensive disproportionation of sodium tetraphenylethylene,[55] although $\Delta H°$ is significantly larger. In both cases, the sign and magnitude of $\Delta S°$ suggest that solvent ordering is the most important solvent effect, and a pair of metal ions in a single molecular unit requires less solvent ordering. It should be noted that our temperature-dependent concentration studies (see Table V) rule out any large temperature variations in TCNE radical concentrations, and this would be more consistent with the very small $\Delta H°$ (-1.3 kcal in THF) obtained for the sodium fluorenone dimer.[54]

One obvious weakness in using these studies to compare with our $TCNE^-$ results (if indeed our anomalous results are due to either of the suggested mechanisms) is that for $TCNE^-$ the relevant equilibrium (5.1) or (5.2) must lie significantly to the left, while in both studies quoted they lie significantly to the right. Clearly further exchange studies, as well as optical and conductance studies would be helpful in resolving the matter.[51,54–56]

An account of further studies of the effects of radical charge and size, solvent, and of ionic strength on Heisenberg exchange rates will be given in Part II of this series.[57] We may note here that it is shown in Part II that the linewidth anomaly of $TCNE^-$ in THF could possibly be due to the deviations of the exchange behavior from the strong-exchange limit. However, the linearity in Fig. 2(b) of the widths vs T/η over a range of a factor of 3 or 4 for T/η, tends to argue against such an explanation. Also, one would expect exchange to be weaker in the solvent having weaker ion pairing,[57] i.e., in DME not in THF.

B. Saturation Studies

The saturation results in Fig. 6 clearly demonstrate the predicted general features of the effects of spin exchange on saturation parameters or (T_1's): their initial decrease with small values of ω_{HE}, but their rapid leveling off with larger values of ω_{HE} to an asymptotic value as given by Eq. (2.28). This is to be compared with the linear decrease in T_2 [or increase in δ as given in Fig. 3(a)] over the same concentration range. In general, then, the effect of exchange is much more pronounced on T_2, with a T_1/T_2 ratio [assuming $T_1(0)=(2W_e)^{-1}$] of

$$\frac{T_{1,\lambda}}{T_{2,\lambda}} = \left[(\tfrac{1}{2}N-D)b''+\frac{T_{1,\lambda}(0)}{T_{2,\lambda}(0)}\right]\left(\frac{1+D_\lambda b''}{1+(N/2)b''}\right), \quad (6.3)$$

[48] A. C. Allen, J. Dieleman, and G. J. Hoijtink, Discussions Faraday Soc. **29,** 182 (1960).

[49] B. J. McClelland, Chem. Rev. **64,** 301 (1964).

[50] N. S. Atherton and S. I. Weissman, J. Am. Chem. Soc. **83,** 133 (1961).

[51] R. H. Boyd and W. D. Phillips, J. Chem. Phys. **43,** 2927 (1965). However, unlike the present proposal, this dimerization was between free ions, not ion pairs, and it was not detectable in solvents other than water. Also, $\Delta H°$ was significantly greater (presumably due to charge repulsions) than in the study reported in Ref. 35 which should be more relevant for comparison with the present case.

[52] We note also that the larger measured value of k for TCNE:THF could, in part, result from an "effective" spin exchange such as

$$K^+TCNE^- + K_2^+TCNE_2^- \rightarrow K_2^+TCNE_2^- + K^+TCNE^-,$$

especially if it were diffusion controlled.

[53] Strictly speaking, these mechanisms would imply that the equilibrium concentration of K^+TCNE^- is not quite a linear function of the initial concentration, although the deviations may not be very large. Thus the results of a concentration-dependent study, like that of Fig. 4, might be expected to yield slight nonlinearities. We have not attempted to include such effects in our analysis.

[54] N. Hirota and S. I. Weissman, J. Am. Chem. Soc. **86,** 2538 (1964).

[55] J. F. Garst, E. R. Zabolotny, and R. S. Cole, J. Am. Chem. Soc. **86,** 2257 (1964); J. F. Garst and E. R. Zabolotny, *ibid.* **87,** 495 (1965).

[56] R. C. Roberts and M. Swarc, J. Am. Chem. Soc. **87,** 5542 (1965).

[57] M. P. Eastman, G. Bruno, and J. H. Freed, "Studies of Heisenberg Exchange in ESR Spectra. II. Effects of Radical Charge and Size," J. Chem. Phys. (to be published).

which increases almost linearly with b'' (or concentration) for moderate to large values of b''.

It is this relatively weak dependence of T_1 on ω_{HE} over a substantial concentration range, coupled with the inherent inaccuracies in T_1 measurements, which makes it difficult to obtain precise quantitative results regarding a detailed comparison between theory and experiment. However, within these limitations, the quantitative results as summarized in Table VI and Fig. 7 are in reasonably good agreement with the theoretical predictions. Even better agreement, at least for the intercepts m (which should be less sensitive to the experimental errors than the slopes a) is achieved when reasonable corrections for END effects are introduced (see Appendix D). One troublesome feature in this study was the extreme narrowness of the very low concentration samples. This made measurements of small changes in linewidths, hence also measurements of saturation parameters, extremely sensitive to error. This specific problem would not be as critical for studies on radicals with significantly greater intrinsic widths.

One obvious lesson to be learned from this work is that linewidth studies are strongly preferred over saturation studies in determining spin-exchange frequencies. On the other hand, saturation studies, by virtue of the different effects exchange has on T_1, can be useful in helping to determine what portion of an observed width is due to exchange. This latter situation can be troublesome, especially with respect to chemical exchange when the chemical composition of the radical sample is not known. Although the present study confined itself to Heisenberg spin exchange, chemical exchange has been predicted to give identical effects for all ESR observables.[13] Thus, in a recent study on the benzene anion,[35] it was possible to rule out the importance of exchange broadening over a part of the temperature range studied, as a result of the observed saturation behavior.

Further matters regarding saturation studies of Heisenberg exchange as well as the application of the ELDOR technique will be discussed in Part III[58] of this series.

APPENDIX A

We utilize Alexander's[20] notation wherein Latin indices (i, j) represent wavefunctions for the exchanging electron spins and Greek indices (α, β) for the rest of the molecule. Then utilizing the exchange property of P we have, in terms of matrix elements,

$$\langle i,\alpha;j,\beta \mid P^x(\rho^{(1)}\cdot\rho^{(2)}) \mid i',\alpha';j',\beta'\rangle = \langle j,\alpha \mid \rho^{(1)} \mid i',\alpha'\rangle\langle i,\beta \mid \rho^{(2)} \mid j',\beta'\rangle - \langle i,\alpha \mid \rho^{(1)} \mid j'\alpha'\rangle\langle j,\beta \mid \rho^{(2)} \mid i',\beta'\rangle. \quad \text{(A1)}$$

Then

$$\langle i,\alpha \,\mathrm{Tr}^{(2)}P^x(\rho^{(1)}\cdot\rho^{(2)}) \mid i',\alpha'\rangle = \sum_j [\langle i \mid \bar{\rho}^{(2)} \mid j\rangle \times \langle j,\alpha \mid \rho^{(1)} \mid i',\alpha'\rangle - \langle i,\alpha \mid \rho^{(1)} \mid j,\alpha'\rangle\langle j \mid \bar{\rho}^{(2)} \mid i'\rangle], \quad \text{(A2)}$$

where

$$\langle i \mid \bar{\rho}^{(2)} \mid j\rangle = \sum_\beta \langle i,\beta \mid \rho^{(2)} \mid j,\beta\rangle$$

etc. Now let

$$N\rho^{(1)} \cong \mathbf{1}^{(1)} + \rho'^{(1)} \quad \text{(A3a)}$$

and

$$N\rho^{(2)} \cong \mathbf{1}^{(2)} + \rho'^{(2)} \quad \text{(A3b)}$$

in the high-temperature approximation.

We now substitute Eqs. (A3) in Eq. (A2) and retain only terms linear in ρ'.[20b] Then

$$N^2\langle i,\alpha \mid \mathrm{Tr}^{(2)}P^x(\rho^{(1)}\cdot\rho^{(2)}) \mid i',\alpha'\rangle \cong \sum_{j\beta} \langle \delta_{ji'}\delta_{\alpha\alpha'}\langle i,\beta \mid \rho'^{(2)} \mid j,\beta\rangle - \delta_{ij}\delta_{\alpha\alpha'}\langle j,\beta \mid \rho'^{(2)} \mid i',\beta\rangle + \langle j,\alpha \mid \rho'^{(1)} \mid i',\alpha'\rangle\delta_{ij} - \delta_{ji'}\langle i,\alpha \mid \rho'^{(1)} \mid k,\alpha'\rangle) = 0. \quad \text{(A4)}$$

APPENDIX B: SATURATION PARAMETERS FOR EXCHANGE[59]

Equations (2.18) and (2.19) are solutions of the matrix equations,

$$(\mathbf{K}+i\mathbf{R})\mathbf{Z} = \mathbf{D}\boldsymbol{\chi}+\mathbf{Q} \quad \text{(B1)}$$

and

$$\mathbf{W}\boldsymbol{\chi} = -2\mathbf{D}^{\mathrm{tr}}\mathbf{Z}'' \quad \text{(B2)}$$

as well as the normalization condition

$$\mathrm{Tr}\boldsymbol{\chi} = 0, \quad \text{(B3)}$$

which is needed because the transition probability matrix $\mathbf{W}$ is always singular. We now redefine a new $\boldsymbol{\chi}$ vector as follows. Let $\chi_{\lambda+}$ and $\chi_{\lambda-}$ correspond to the $M_s=+$ and $-$ states constituting the λth transition. Then $\hat{X}_\lambda \equiv \chi_{\lambda+}-\chi_{\lambda-}$. Thus, while $\boldsymbol{\chi}$ has N components, $\hat{X}$ has $\frac{1}{2}N$ components. Similarly we define a $\frac{1}{2}N$-dimensional square matrix $\hat{\mathbf{W}}$ (which is usually nonsingular) according to

$$[\hat{\mathbf{W}}\hat{X}]_\lambda \equiv [\mathbf{W}\boldsymbol{\chi}]_{\lambda+} - [\mathbf{W}\boldsymbol{\chi}]_{\lambda-}. \quad \text{(B4)}$$

One can test whether the definition [Eq. (B4)] is a meaningful one by expanding the elements of $\mathbf{W}\boldsymbol{\chi}$ etc., in Eq. (B4). One finds that two independent conditions of the transition probabilities must be fulfilled,

$$(W_{\alpha+\gamma+} - W_{\alpha+\gamma-}) = (W_{\alpha-\gamma-} - W_{\alpha-\gamma+}), \qquad \alpha \neq \gamma, \quad \text{(B5a)}$$

[58] M. P. Eastman, G. Bruno, and J. H. Freed, "Studies of Heisenberg Exchange in ESR Spectra. III. An ELDOR Study," J. Chem. Phys. (to be published).

[59] We wish to acknowledge the aid of Daniel S. Leniart in obtaining some of the results in this Appendix.

and

$$(2W_{\gamma+\gamma-}+\sum_{\alpha\pm\neq\gamma\pm}W_{\gamma+\alpha\pm})=(2W_{\gamma-\gamma+}+\sum_{\alpha\pm\neq\gamma\pm}W_{\gamma-\alpha\pm}). \quad \text{(B5b)}$$

The first term on each side of Eq. (B5a) corresponds to the W_n for $M_s=+$ and $-$, while the second corresponds to the W_x. They are both included in the summation of terms on both sides of Eq. (B5b) which also has terms corresponding to W_e on each side. The conditions (1) and (2) given in Sec. II are a reasonable set of sufficient conditions for Eqs. (B5) to hold. We still must see how exchange processes permit the definition of (B4). This can best be done by starting with Eq. (2.18) of Ref. 13,

$$[\mathbf{W}_{EX}\chi]_{\alpha\pm}=\omega_{EX}[\tfrac{1}{2}(\chi_{\alpha\pm}-\chi_{\alpha\pm})+\chi_{\pm}], \quad \text{(B6)}$$

where

$$\chi_{\pm}=(2/N)\sum_{\gamma}\chi_{\gamma\pm}. \quad \text{(B6')}$$

Thus from Eqs. (B6a) and (B3),

$$\chi_{+}+\chi_{-}=0. \quad \text{(B6'')}$$

Then

$$[\mathbf{W}_{EX}\chi]_{\alpha+}-[\mathbf{W}_{EX}\chi]_{\alpha-}=\omega_{EX}[(\chi_{\alpha-}-\chi_{\alpha+})+(\chi_{+}-\chi_{-})]=-\omega_{EX}\{[1-(2/N)]\hat{\chi}_{\alpha}-\sum_{\gamma\neq\alpha}(2/N)\hat{\chi}_{\gamma}\}, \quad \text{(B7)}$$

where Eqs. (B6) were used to obtain the second equality of Eq. (B7), which has the proper form. Also, for exchange processes we note

$$[\mathbf{W}_{EX}\chi]_{\alpha+}+[\mathbf{W}_{EX}\chi]_{\alpha-}=\omega_{EX}[\chi_{+}+\chi_{-}]=0. \quad \text{(B8)}$$

Finally, to obtain the simplified solution to Eqs. (B1) and (B2), one must introduce a transition moment matrix $\mathbf{D}$ of order $\frac{1}{2}(M\times N)$ (where M equals the number of induced transitions) instead of $\mathbf{D}$ of order $M\times N$, so that Eqs. (B1) and (B2) become

$$(\mathbf{K}+i\mathbf{R})\mathbf{Z}=\hat{\mathbf{D}}X+\mathbf{Q} \quad \text{(B9a)}$$

and

$$\hat{\mathbf{W}}X=-4\hat{\mathbf{D}}^{\mathrm{tr}}\mathbf{Z}''. \quad \text{(B9b)}$$

Equstions (2.18)–(2.20) are again the correct solution, but now we have

$$\mathbf{S}=4\hat{\mathbf{D}}(\hat{\mathbf{W}})^{-1}\hat{\mathbf{D}}^{\mathrm{tr}}, \quad \text{(B10)}$$

when only ESR transitions are excited. Thus, any particular spin eigenstate is involved in no more than one induced transition; so

$$S_{\lambda j,\eta k}=4d_{\lambda_j}d_{\eta_k}(W^{-1})_{\lambda_j\eta_k}=d_{\lambda_j}d_{\eta_k}\Omega_{\lambda_j,\eta_k}. \quad \text{(B11)}$$

Equation (B11) involves the inversion of a $\frac{1}{2}N\times\frac{1}{2}N$ nonsingular matrix instead of the $N\times N$ singular $\mathbf{W}$ matrix [plus Eq. (B3)].

It is now possible, in the presence of degeneracies, to further simplify by summing over the degenerate transitions and over degenerate states [see Eqs. (2.22)] under appropriate conditions as discussed in Sec. II an in fuller detail in Ref. 13. We again assume that the dominant nuclear-spin-dependent relaxation terms are the exchange processes, so utilizing Eqs. (3.23) of Ref. 13 we have for the general case in units of W_e

$$\hat{W}'=\begin{pmatrix} 2D_a(1+[N/2-D_a]b'') & -2D_aD_bb'' & \cdots & -2D_aD_nb'' \\ -2D_bD_ab'' & 2D_b(1+[N/2-D_b]b'') & \cdots & -2D_bD_nb'' \\ -2D_eD_ab'' & -2D_eD_bb'' & \cdots & -2D_eD_nb'' \\ \vdots & \vdots & & \vdots \\ -2D_nD_ab'' & -2D_nD_bb'' & \cdots & 2D_n(1+[N/2-D_n]b'') \end{pmatrix}. \quad \text{(B12)}$$

Let c_{ij} be the ijth element of $\hat{W}'$ and C_{ij} its cofactor. Then

$$(\hat{W}'^{-1})_{aa}=C_{aa}/\sum_{i}c_{ai}C_{ai}. \quad \text{(B13)}$$

Now consider the cofactor C_{aa} of Eq. (B12). By summing all rows on the first, recognizing that $\sum_i D_i=\frac{1}{2}N$, and extracting common multipliers of rows and columns one has

$$C_{aa}=2(1+b''D_a)D_b[D_eD_d\cdots D_n]^2\begin{vmatrix} 1 & 1 & \cdots & 1 \\ -2b'' & 2[1+(\frac{1}{2}N-D_e)b''] & \cdots & -2b'' \\ \vdots & \vdots & & \vdots \\ -2b'' & -2b'' & \cdots & 2[1+(\frac{1}{2}N-D_n)b''] \end{vmatrix}. \quad \text{(B14)}$$

Let us denote the determinant on the right of Eq. (B14) by $|A|$. In a similar manner one can show

$$C_{ai}=2b''D_aD_b[D_cD_d\cdots D_n]^2\,|A|, \qquad i\neq a. \tag{B14'}$$

Then

$$(\hat{W}'^{-1})_{aa}=\frac{2(1+b''D_a)}{4D_a(1+b''D_a)(1+[\frac{1}{2}N-D_a]b'')-4D_a^2b''^2\sum_{i\neq a}D_i}$$
$$=(2D_a)^{-1}\{(1+D_ab'')/[1+(\tfrac{1}{2}N)b'']\}. \tag{B15}$$

Now, since "a" can represent any hyperfine transition, we obtain Eq. (2.26) from Eqs. (B15) and (B11). In a similar manner one may derive a general relationship for the cross-saturation parameter between the ith and jth transitions, which is important in ELDOR, as

$$\Omega_{i,j}=(2/W_e)\{b''/[1+(\tfrac{1}{2}N)b'']\}, \qquad i\neq j. \tag{B16}$$

It is thus independent of the degeneracies of these transitions.

APPENDIX C: INTERMOLECULAR ELECTRON SPIN–DIPOLAR INTERACTIONS IN SOLUTION

The Effect of Electron Delocalization

The theory of nuclear-spin relaxation from intermolecular nuclear-spin dipolar interactions, in which the nuclei may be treated as point dipoles, is well developed.[60] It is less clear that predictions for point dipoles apply to intermolecular electron spin–dipolar interactions, since the electrons are delocalized in orbitals. In the following we discuss the effect of electronic delocalization on the dipolar interaction for the simple case of two electrons in P orbitals. It is shown that at the radical-separation distances estimated for the $TCNE^-$ experiments the point-dipole approximation is probably valid.

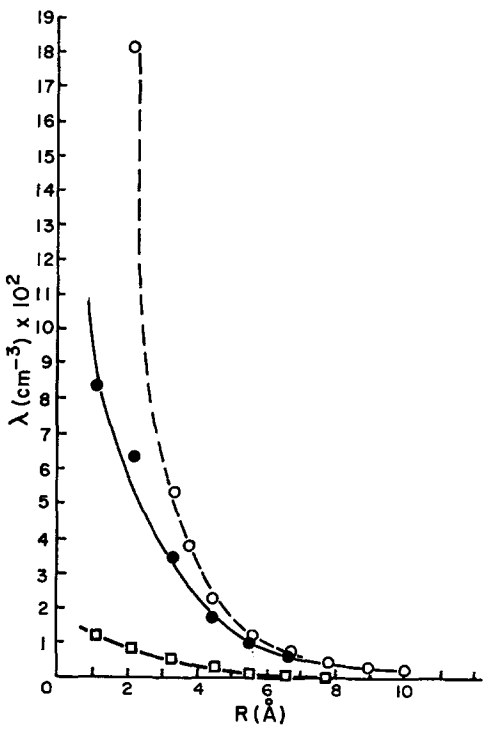

FIG. 8. λ and μ as functions of R for two interacting dipoles. Here ○ represents λ for point dipoles, while ● and □ represent λ and μ, respectively, for dipoles delocalized in separate P orbitals. For the two point dipoles, R is the distance between dipoles, while for two dipoles delocalized in P orbitals, R is the distance between centers of the P orbitals.

The problem of electron spin–dipolar interactions between two electrons in carbon $2P$ orbitals has been studied by Gouterman and Moffitt.[61] The spin Hamiltonian is

$$\mathcal{H}=[D(S_z^2-\tfrac{1}{3}\mathbf{S}^2)+E(S_x^2-S_y^2)], \tag{C1}$$

where $\mathbf{S}=\mathbf{S}_1+\mathbf{S}_2$. Gouterman and Moffitt's parameters λ and μ are just $\lambda=-4/3(g\beta)^{-2}D$ and $\mu=-4(gB)^{-2}E$. One then has for the point-dipole case,

$$\lambda=2/r_{12}^3, \qquad \mu=0, \tag{C2}$$

while for the general case[61,62]

$$\lambda=\iint\psi_T^*\left(\frac{3z_{12}^2-r_{12}^2}{r_{12}^5}\right)\psi_T dv_1dv_2,$$
$$\mu=\iint\psi_T^*\left(\frac{3x_{12}^2-3y_{12}^2}{r_{12}^5}\right)\psi_T dv_1dv_2, \tag{C3}$$

where ψ_T is the total orthonormalized orbital wavefunction for the system of two electrons. The results for a point dipole as given by Eq. (C2) and for the valence-bond antisymmetric orbital component[63] obtained by Gouterman and Moffitt (who utilized Gaussian orbitals) are compared as a function of the internuclear distance R in Fig. 8. It is seen that $\lambda>\mu$ in both cases. Both values for λ and both for μ approach each other for $R>4$ Å, partly because the effective overlap of the P orbitals for a separation greater than 4 Å is small.[61] Thus, in the region of small overlap, two electrons in P orbitals appear to interact like two point dipoles. In

[60] A. Abragam, *The Principles of Nuclear Magnetism* (Oxford University Press, London, 1961).

[61] M. Gouterman and W. Moffitt, J. Chem. Phys. **30**, 1107 (1959).

[62] A. Carrington and A. D. McLachlan, *Introduction to Magnetic Resonance* (Harper and Row Publishers, Inc., New York, 1967).

[63] It is easy to show that the dipolar interactions of pairs of doublets (such as what occurs for dilute solutions of free radicals) is determined solely by the antisymmetric orbital component since, the symmetric component is diamagnetic.

TABLE VIII. Effect of dipolar interactions on least-squares slope and intercept for the fit of the exchange data to

$$\delta = g(T/\eta) + \delta(T/\eta = 0).^{a}$$

Dipolar correction	C (moles/liter)	g(G·cP/°K$\times 10^4$)	$\delta(T/\eta=0)$ (G)
Uncorrected	3×10^{-5}	−0.08	0.021
Uncorrected	2.5×10^{-3}	8.99	0.027
Corrected	2.5×10^{-3}	9.31	0.013

[a] All values are for the $\bar{M}=0$ line.

the region $R<4$ Å the strength of the dipolar interaction as evidenced by λ is weaker in the case of overlapping P electrons. This is because electron correlation, implicit in the valence-bond wavefunction, keeps the electrons away from each other.

The Relative Importance of Dipolar Interactions and Heisenberg Exchange

The calculation of the effect of dipolar interactions on the transverse relaxation time T_2 is based on the point-dipole results summarized by Abragam.[60] The dipolar interaction between two radicals with differing nuclear configurations is considered as an interaction between two unlike spins, while those between radicals with the same nuclear configuration are considered to be between like spins. They yield width contributions of $(T_2)_1^{-1}$ and $(T_2)_2^{-1}$, respectively. This separation is appropriate as long as $|\omega^D{}_E| \ll |a|$. One has

$$(T_2)_1^{-1} = \hbar^2\gamma^4 S(S+1)[(\tfrac{1}{2}N - D_M)/\tfrac{1}{2}N]\{\tfrac{1}{6}J^{(0)}(0) + (1/24)J^{(0)}[a(M-M')] + \tfrac{3}{4}J^{(1)}(\omega_e) + \tfrac{3}{2}J^{(1)}(\omega_e) + \tfrac{3}{8}J^{(2)}(2\omega_e)\}, \quad \text{(C4a)}$$

$$(T_2)_2^{-1} = \hbar^2\gamma^4 S(S+1)(2D_j/N) \times [\tfrac{3}{8}J^{(2)}(2\omega_e) + (15/4)J^{(1)}(\omega_e) + \tfrac{3}{8}J^{(0)}(0)]. \quad \text{(C4b)}$$

$J^{(i)}(\omega)$ is the spectral density at frequency ω of the ith random time function that appears in the expansion of the random Hamiltonian $\mathcal{H}_1$.[60] The appropriate correlation time τ for the relative translational diffusion of two radicals is in a Stokes–Einstein approximation[60] (neglecting charge effects)

$$\tau = 12\pi a^3\eta/kT = 3\tau_1. \quad \text{(C5)}$$

One finds that $\tau \gtrsim 10^{-10}$ if $a \gtrsim 2$ Å and η/T of the order expected for DME. The following approximations for the spectral density function at microwave frequencies can then be made[60,64]:

$$J^{(0)}[a(M-M')] \backsim J^{(0)}(0), \quad J^{(1)}(\omega_e), J^{(2)}(2\omega_e) \ll J^{(0)}(0), \quad \text{(C6)}$$

where $J^{(0)}(0)$ is[60]

$$J^{(0)}(0) = 32\pi^2\mathfrak{N}\eta/25kT. \quad \text{(C7)}$$

Now from Eqs. (2.15) and (2.16) we have for strong exchange (neglecting charge effects)

$$(T_2)_{\mathrm{HE}}^{-1} = [(\tfrac{1}{2}N - D_M)/\tfrac{1}{2}N](\mathfrak{N}kT/\eta)^{\frac{4}{3}}. \quad \text{(C8)}$$

Thus from Eqs. (C4)–(C8) one has

$$[(T_2)^{-1}\text{dipole}]_M/[(T_2)^{-1}\text{exchange}]_M = K_M(\eta/kT)^2, \quad \text{(C9)}$$

where

$$K_M = \hbar^2\gamma^4 S(S+1)\pi^2/25[(5N-8D_M)/(N-2D_M)],$$

and Eq. (C9) is independent of concentration.

Table VIII shows the effect of the dipolar corrections on the least-squares slope and intercept for the $\bar{M}=0$ line of TCNE of Fig. 2(a). It is seen that dipolar interactions as calculated here have only a negligible (within experimental error) effect on the experimentally determined exchange rates.

APPENDIX D

Effects of Weak END Interactions on the Exchange-Saturation Studies

Here we assume the END-induced nuclear spin-flip rate ${}^{W}N^{(D)} = \tfrac{1}{2}j_N{}^D(0) \neq 0$, but $b \equiv {}^{W}N^{(D)}/W_e \ll 1$. Thus for all values of ω_{HE}, it is possible to regard each multiple hyperfine line as an average Lorentzian even with regard to its saturation behavior.[13,28] We now make use of the methods of Appendix B in a simple way. We must add the effects of $W_N{}^{(D)}$ to the $\hat{W}'$ matrix as given by Eq. (B12). One finds using methods of Ref. 13 that for the off-diagonal elements,

$$-\hat{W}_N{}^{(D)\prime}(M, M\pm1) = b\sum_j [J_j(J_j+1) - M(M\pm1)] \quad \text{(D1)}$$

in units of W_e, where the sum over j is a sum over all the components of the multiple hyperfine line corresponding to a particular value of M. The diagonal elements are obtained by noting that a sum over each row (or column) of W' must equal zero for terms in b.

When the terms from Eq. (D1) are inserted into Eq. (B12), it is possible to obtain a simple solution to Eq. (B13) when $b'' \ll 1$. (This is also the region where a nonnegligible $b \ll 1$ will have its most significant effects.) To obtain results first order in b and b'' it is necessary only to retain the diagonal elements of the matrix in Eq. (B12) [including terms from Eq. (D1)]. One then has

$$\Omega_\lambda \cong (2/W_e D_\lambda)[1 - (\tfrac{1}{2}N - D_\lambda)b'' - \epsilon_\lambda], \quad \text{(D2a)}$$

where

$$\epsilon_\lambda = (b/D_\lambda)\sum_{j \text{ in } \lambda}[J_j(J_j+1) - M^2], \quad \text{(D2b)}$$

[64] C. P. Slichter, *Principles of Magnetic Resonance* (Harper and Row Publishers, Inc., New York, 1963).

which agrees with Eq. (2.26) for $b=0$ and $b''\ll 1$. Now the asymptotic limit for Eq. (2.26) when $b''\gg 1$ cannot be affected by finite values of b, since both END and exchange terms have the same qualitative effects on Ω_λ.[13,19] These two limits may then be incorporated into a revised form of Eq. (2.26),

$$\Omega_\lambda=\Omega_\lambda(b'', b=0)[(1-\epsilon_\lambda)+D_\lambda b'']/(1+\tfrac{1}{2}Nb'')]. \quad \text{(D3)}$$

Equation (5.6) then becomes

$$[1-T_{1,\bar{M}}/T_1, (0)]^{-1} = [1+(\tfrac{1}{2}N)b'']/[\epsilon_{\bar{M}}-(\tfrac{1}{2}N-D_{\bar{M}})b''], \quad \text{(D4)}$$

which no longer has a simple linear dependence on b''^{-1}. [In Eq. (D4), $T_1(0)=(2W_e)^{-1}$.] However, the analysis in Sec. V was based on finding that value of $T_1(0)$ which gives the best *linear fit* to the data. If we let $\tilde{T}_{1,\bar{M}}(0)\equiv[T_1(0)](1-\epsilon_{\bar{M}})$, so that $\tilde{T}_{1,\bar{M}}(0)$ is the concentration-independent value found experimentally for $\epsilon_{\bar{M}}\neq 0$, and if we recognize that b'' obtained utilizing this value of $\tilde{T}_{1,\bar{M}}(0)$ in place of $T_1(0)$ is not strictly that defined by Eq. (5.1) [call it $\tilde{b}''=(1-\epsilon)b''$] then we have

$$[1-T_{1,\bar{M}}/\tilde{T}_{1,\bar{M}}(0)]^{-1}=\tilde{m}\tilde{b}''^{-1}+\tilde{a}, \quad \text{(D5)}$$

where

$$\tilde{m}=(1-\epsilon)^2[(\tfrac{1}{2}N)(1-\epsilon)-D_{\bar{M}}]^{-1}$$

and

$$\tilde{a}=[1-2D_{\bar{M}}/N(1-\epsilon)]^{-1}.$$

END Effects in TCNE

A careful analysis of the derivative widths of the hyperfine lines, utilizing their relative intensities, was made for a $3\times10^{-5}M$ solution of $TCNE^-$ in DME at 15°C. The results may be summarized as

$$\delta(\bar{M})=(22.5\pm0.09)+(0.16\pm0.04)\bar{M} + (0.28\pm0.01)\eta(\bar{M}_N)\ \text{mG}, \quad \text{(D6)}$$

where $\eta(0)=0$, $\eta(\pm1)=2.693$, $\eta(\pm2)=10.393$, $\eta(\pm3)=23.526$, and $\eta(\pm4)=41.193$. Equation (D6) was determined from just the $\bar{M}=0$, ±1, and ±2 lines. The results are nearly the same when the ±3 lines are included, although these lines may be somewhat distorted by overlapping ^{13}C splittings.[14] Equation (D6) is of the form appropriate when the END effects are small, and each line is an average Lorentzian,[14] which is reasonably justified by the weak dependence on $\eta(\bar{M}_N)$. It is to be compared with the theoretical result[14,28]

$$\langle T_2^{-1}(M)\rangle=j^D(0)\eta(M)+(16/3)j^{(DG)}(0)B_0M+X, \quad \text{(D7)}$$

which is valid when nonsecular END and g-tensor linewidth contributions are negligible.[14,28] A comparison of Eqs. (D6) and (D7) leads to the result $j^D(0)=4.26\times10^3\ \text{sec}^{-1}$. When the nominal value of $T_1(0)\sim 7\times10^{-6}$sec is used, one obtains from Eq. (D2b) $\epsilon_{M=0}=0.164$. This should be regarded as a crude estimate[65] but sufficient for present purposes. Table IX gives the values of $\tilde{m}$ and $\tilde{a}$ from Eq. (D5) calculated for $\bar{M}=0$ for different values of $\epsilon_{M=0}$. It is seen that the effect of a finite ϵ_0 is to significantly improve the agreement with the experimentally determined value of the intercept a (Table VI). The uncertainty in the experimental value of m is beyond the small variation of $\tilde{m}$ in Table IX, but these results are consistent with the best estimate of $\tilde{T}_{1,\bar{M}}(0)$ (from Table VI) being about $6.5\text{–}7.0\times10^{-6}$ sec. Similar remarks apply for nonzero values of ϵ_{-1} and ϵ_{-2}.

TABLE IX. Predicted corrections to the concentration-dependent saturation behavior resulting from weak END interactions.

$\bar{M}$	$\epsilon_{\bar{M}}$	$m\times10^2$ [a]	$\tilde{a}$ [a]
0	0	1.61	1.31
	0.1	1.50	1.35
	0.2	1.40	1.42
−1	0	1.54	1.247
	0.1	1.44	1.28
	0.2	1.31	1.33
−2	0	1.41	1.14
	0.1	1.29	1.16
	0.2	1.17	1.18

[a] Parameters defined in Appendix D.

[65] One may estimate τ_R for the rotational tumbling, and one finds $\omega_e\tau_R\sim1.5$ [M. R. Das and J. H. Freed (unpublished)]. Thus, the neglect of nonsecular terms in Eq. (D7) is not completely justified. However, these terms should have comparable effects on both the widths and the parameter to be estimated $\epsilon_{\bar{M}}$. (Their effect on the saturation behavior is *not* readily calculated by the methods of Appendix B.) Thus, this should not significantly affect the order-of-magnitude nature of our estimates of $\epsilon_{\bar{M}}$.